# DESIGN OF OPTIMAL MANEUVERING CONTROL OF THE 3000 TON SURFACE EFFECT SHIP DURING FAILURE MODES

Spyridon Michael-Dionyssios Manoussos

# NAVAL POSTGRADUATE SCHOOL
## Monterey, California


# THESIS

Design of Optimal Maneuvering Control
of the 3000 Ton Surface Effect Ship
During Failure Modes

by

Spyridon Michael-Dionyssios Manoussos

December 1979

Thesis Advisor: A. Gerba

Approved for public release; distribution unlimited

SECURITY CLASSIFICATION OF THIS PAGE (When Data Entered)

| REPORT DOCUMENTATION PAGE | | READ INSTRUCTIONS BEFORE COMPLETING FORM |
|---|---|---|
| 1. REPORT NUMBER | 2. GOVT ACCESSION NO. | 3. RECIPIENT'S CATALOG NUMBER |
| 4. TITLE (and Subtitle)<br>Design of Optimal Maneuvering Control of the 3000 Ton Surface Effect Ship During Failure Modes | | 5. TYPE OF REPORT & PERIOD COVERED<br>Master's Thesis; December 1979<br>6. PERFORMING ORG. REPORT NUMBER |
| 7. AUTHOR(s)<br>Spyridon Michael-Dionyssios Manoussos | | 8. CONTRACT OR GRANT NUMBER(s) |
| 9. PERFORMING ORGANIZATION NAME AND ADDRESS<br>Naval Postgraduate School<br>Monterey, California 93940 | | 10. PROGRAM ELEMENT, PROJECT, TASK AREA & WORK UNIT NUMBERS |
| 11. CONTROLLING OFFICE NAME AND ADDRESS<br>Naval Postgraduate School<br>Monterey, California 93940 | | 12. REPORT DATE<br>December 1979<br>13. NUMBER OF PAGES |
| 14. MONITORING AGENCY NAME & ADDRESS(if different from Controlling Office) | | 15. SECURITY CLASS. (of this report)<br>UNCLASSIFIED<br>15a. DECLASSIFICATION/DOWNGRADING SCHEDULE |
| 16. DISTRIBUTION STATEMENT (of this Report)<br>Approved for public release; distribution unlimited | | |
| 17. DISTRIBUTION STATEMENT (of the abstract entered in Block 20, if different from Report) | | |
| 18. SUPPLEMENTARY NOTES | | |
| 19. KEY WORDS (Continue on reverse side if necessary and identify by block number)<br>Optimal Control, Surface Effect Ship Simulation | | |

20. ABSTRACT (Continue on reverse side if necessary and identify by block number)

A simplified form of the three-degrees-of-freedom nonlinear equations of the 3000 ton Surface Effect Ship (SES) was linearized around an equilibrium point when a thruster failure or thruster reversal occured. Optimal control feedback gains were calculated with the linearized system and applied to the nonlinear system. Evaluation of this design was based upon both comparison of the real-time human operator response and additionally a state feedback design based upon a trial and error procedure.

DD FORM 1 JAN 73 1473 EDITION OF 1 NOV 65 IS OBSOLETE
S/N 0102-014-6601

(Page 1)



SECURITY CLASSIFICATION OF THIS PAGE (When Data Entered)

# Design of Optimal Maneuvering Control of the 3000 Ton Surface Effect Ship During Failure Modes

by

Spyridon Michael-Dionyssios Manoussos
Lieutenant, Hellenic Navy
B.S.E.E., Naval Postgraduate School, 1979

Submitted in partial fulfillment of the requirements for the degree of

MASTER OF SCIENCE IN ELECTRICAL ENGINEERING

from the

NAVAL POSTGRADUATE SCHOOL
December 1979

ABSTRACT

A simplified form of the three-degrees-of-freedom nonlinear equations of the 3000 ton Surface Effect Ship (SES) was linearized around an equilibrium point when a thruster failure or thruster reversal occured. Optimal control feedback gains were calculated with the linearized system and applied to the nonlinear system. Evaluation of this design was based upon both comparison of the real-time human operator response and additionally a state feedback design based upon a trial and error procedure.

TABLE OF CONTENTS

LIST OF TABLES

LIST OF FIGURES

ACKNOWLEDGEMENT

The author wishes to express his sincere appreciation to Associate Professor Alex Gerba, Jr. of the Naval Postgraduate School for his assistance and continuous guidance during the pursuit of this study.

The author also wishes to acknowledge the many persons to whom he is indebted for their assistance in the preparation of this work. Significant appreciation must be extended to Major T. S. Nelson, USMC, who devoted many hours in assisting the preparation of this effort.

# I. INTRODUCTION

Over the past years a lot of attention has been given to the Surface Effect Ship (SES) due to its advantages over conventional ship designs [Refs. 1, 2, and 3]

Recent investigations regarding water jet propulsion SES have been conducted on the computer assisted mode of operation either in a normal mode of operation or during a variety of failures [Ref. 3]. Failures considered include, among others, complete loss of thrust and reversal of thrust of a nozzle.

The purpose of this thesis was to investigate the possibility of optimal maneuvering of a 3000 ton Surface Effect Ship during the above mentioned emergencies.

As discussed in [Ref. 3], turn maneuvers for the 3KSES are the result of turning moments generated by modulating the waterjet thrust vectors. This modulation is achieved by a combination of thrust amplitude modulation (controlled by varying the flow rates of the four waterjets to create a net differential thrust, i.e., by varying the power turbine speeds of the individual propulsion engines), and thrust vectoring (controlled by varying the directions of the four waterjet deflection sleeves).

In the computer assist mode, the relative position of the helm determines the angular rate at which the turn is negotiated. Full helm position corresponds to the maximum safe

turning rate for a given ship speed. Calibration of the helm input is done within the control computer, which then generates commands to the individual control effectors to produce the commanded turn rate.

In the manual mode, the relative helm position generates commands for the direction nozzles directly. A common position command drives all four deflection sleeves. Because of that, the rate of turn which corresponds to a particular helm position is dependent on the hydrodynamic yawing moment which is a function of ship speed. The operator can also generate a thrust differential turning moment in the manual mode by proper selection of the propulsion engine control levers.

To relieve the operator of the work load related to monitoring and maintaining ship heading over extended periods of time, a heading control autopilot is included in the design of the heading control system. From an operational point of view, the heading autopilot is limited to a "heading hold" function, and is used only in conjunction with the computer assist mode of operation. The net result of this operation is that the heading autopilot replaces the operator's hand on the helm, while the helm is still the primary control input device for the control of ship heading.

This is accomplished by direct feedback of the yaw rate to a processor which also gets an error channel from the autopilot through a control filter using proportional plus integral control of the heading angle.

The fundamental optimality requirement used in [Ref. 2] is concerned with minimizing fuel and effector duty cycle while executing prescribed maneuvers. This was done by minimization of a function of the state variables.

The approach used in this work was to achieve results by minimizing a functional of the form $\int_{to}^{tf} (\underset{\sim}{x}^T \underset{\sim\sim}{Q} \underset{\sim}{x} + \underset{\sim}{\mu}^T \underset{\sim\sim}{R} \underset{\sim}{\mu}) dt$ to compute the gains for the state feedback control (see Appendix A).

The resulting linear regulator design was tested on the nonlinear system to compare the performance of the craft during a failure mode with the performance of a human operator using a real time simulation [Ref. 4]. The performance of the design during a failure was also compared with a corrective algorithm for control found by simple trial and error procedures.

## II. EQUATIONS OF MOTION OF THE THREE-DEGREE-OF FREEDOM (3DOF) MODEL

The three degrees of freedom to be used in this analysis are: surge, sway and yaw [Ref. 5]. Therefore, the following assumptions and approximations were made:

1. Roll is zero.

2. Pitch and draft remain constant.

3. The origin of the ship's coordinate system is located at the center of gravity of the ship.

4. At time = 0, the ship's coordinate system and the fixed (geographical) coordinate system have the same origin and the same coordinate axes, i.e., $x_{NAV} = x_o = 0$ and $y_{NAV} = y_o = 0$ (see Fig. 1).

5. At time = 0 the ship is heading in the positive $x_{NAV}$ direction.

6. Drift angle subtraction effect on thrust angle is zero.

Then, as a good approximation, the equations of motion are:

Surge: $m(\dot{u}-vr) = X$ (1)

Sway: $m(\dot{v}+ur) = Y$ (2)

Yaw: $I_z\dot{r}=N$ (3)

Navigation:

$$\dot{x}_o = u\cos\psi - v\sin\psi \quad (4)$$

$$\dot{y}_o = u\sin\psi + v\cos\psi \quad (5)$$

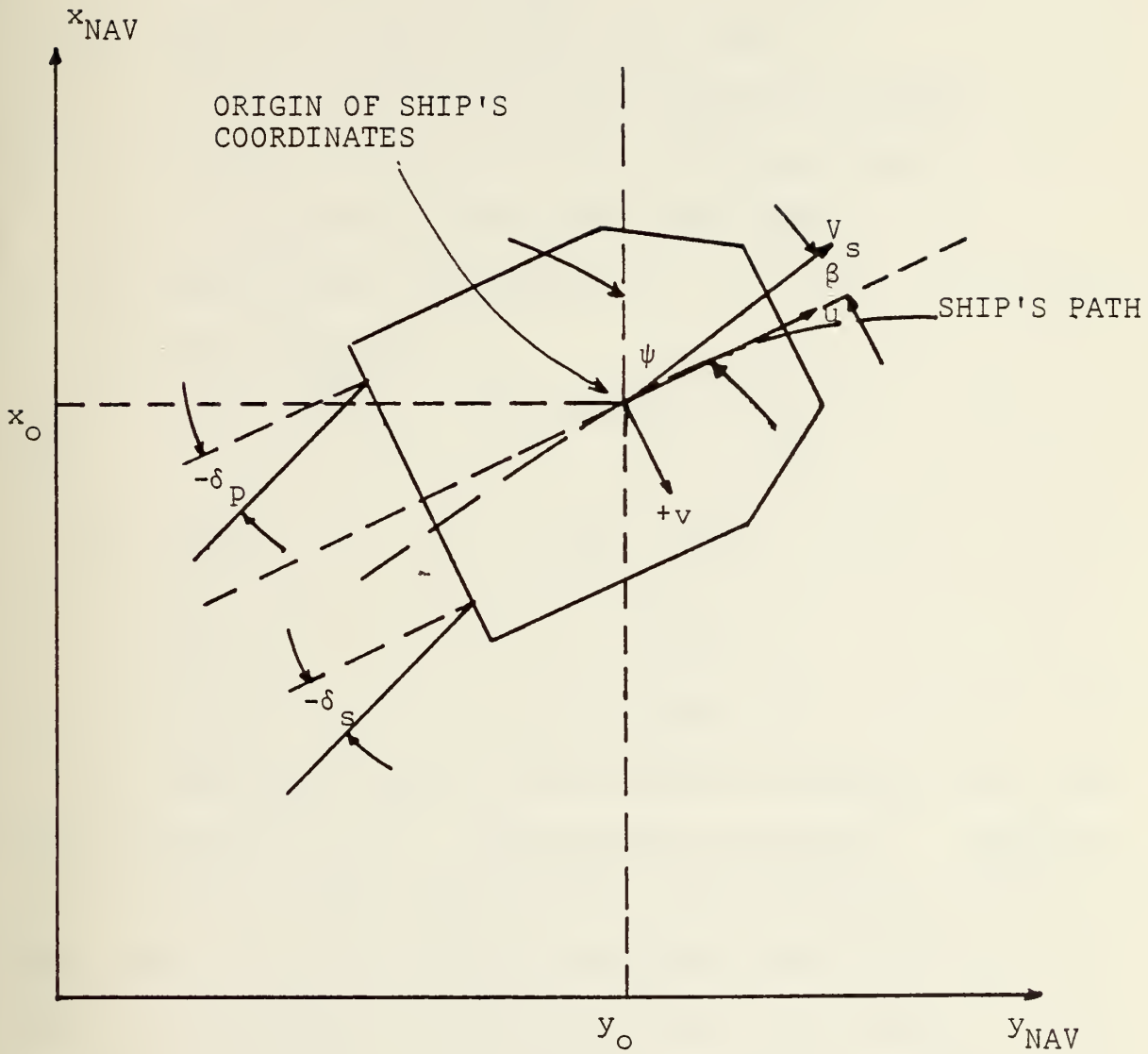


Fig. 1 - Definition of Coordinate System

NOTE: Rudder condition for right turn is shown. All runs start at geographic origin.

$$V_s = \sqrt{u^2+v^2} \tag{6}$$

$$\beta = \tan^{-1}\left(\frac{-v}{u}\right) \tag{7}$$

In the above equations:

$m$ = mass of the rigid ship

$I_z$ = moment of inertia about the z axis

$u = V_s\cos\beta$ = velocity in the x direction (Surge)

$v = V_s\sin\beta$ = velocity in the y direction (Sway)

$r = \dot{\psi}$ = angular velocity about the z axis

$\psi$ = heading (yaw) angle, Fig. 1

$\beta$ = drift angle, Fig. 1

$\delta$ = rudder angle, $+\delta$ produces a left turn

Also:

$$x_o = \int \dot{x}_o dt \qquad y_o = \int \dot{y}_o dt$$

$$u = \int \dot{u} dt \qquad v = \int \dot{v} dt$$

$$r = \int \dot{r} dt \qquad \psi = \int \dot{\psi} dt$$

The right-hand side of the equations of motion have been represented by X, Y, N. These symbols represent: summation of forces (X, Y) and moments (N). Each summation consists of many terms. For the initial simplified model, only the few terms that are major contributions have been retained. Those terms are considered sufficient to produce a simulation which would be in close agreement with obtained data. At a later time, the model may be improved by adding more terms and adjusting coefficients.

After reduction of the right-hand-sides, these force and moment summations become:

$$X = GT\cos\delta - C_{DX}u^2 \tag{8}$$

$$Y = GT\sin\delta - C_{DY}v|v| \tag{9}$$

$$N = -(GT\sin\delta)l_o + C_{DY}v|v|l_w \tag{10}$$

where (see Fig. 2):

GT = gross thrust in lbs.

$\delta = \delta_s = \delta_p$ = angle of all thrust vectors (starboard and port) in radians

$C_{DX}$ = coefficient of drag in the direction of surge

$C_{DY}$ = coefficient of drag in the direction of sway

$l_o$ = thrust level arm in feet

$l_w$ = sway-drag level arm in feet

Also, note that the drag forces have been chosen as lumped parameters acting at the two points P & P', i.e. P & P' are equivalent force centroids.

The length $l_o$ is the distance from the center of gravity to the stern, and $l_w$ is the distance (in the x-direction) from the center of gravity to the points P & P'. $l_o$ is taken as a fixed parameter (it could be charged by various conditions of ship loading) but $l_w$ is adjustable in order to be used as a parameter to make the model fit test data.

The coefficient $C_{DX}$ in eq. 8 is a lumped parameter equivalent for the hull friction effect (slender body theory). The term $C_{DX}u^2$ models the hull drag, aerodynamic and hydrodynamic

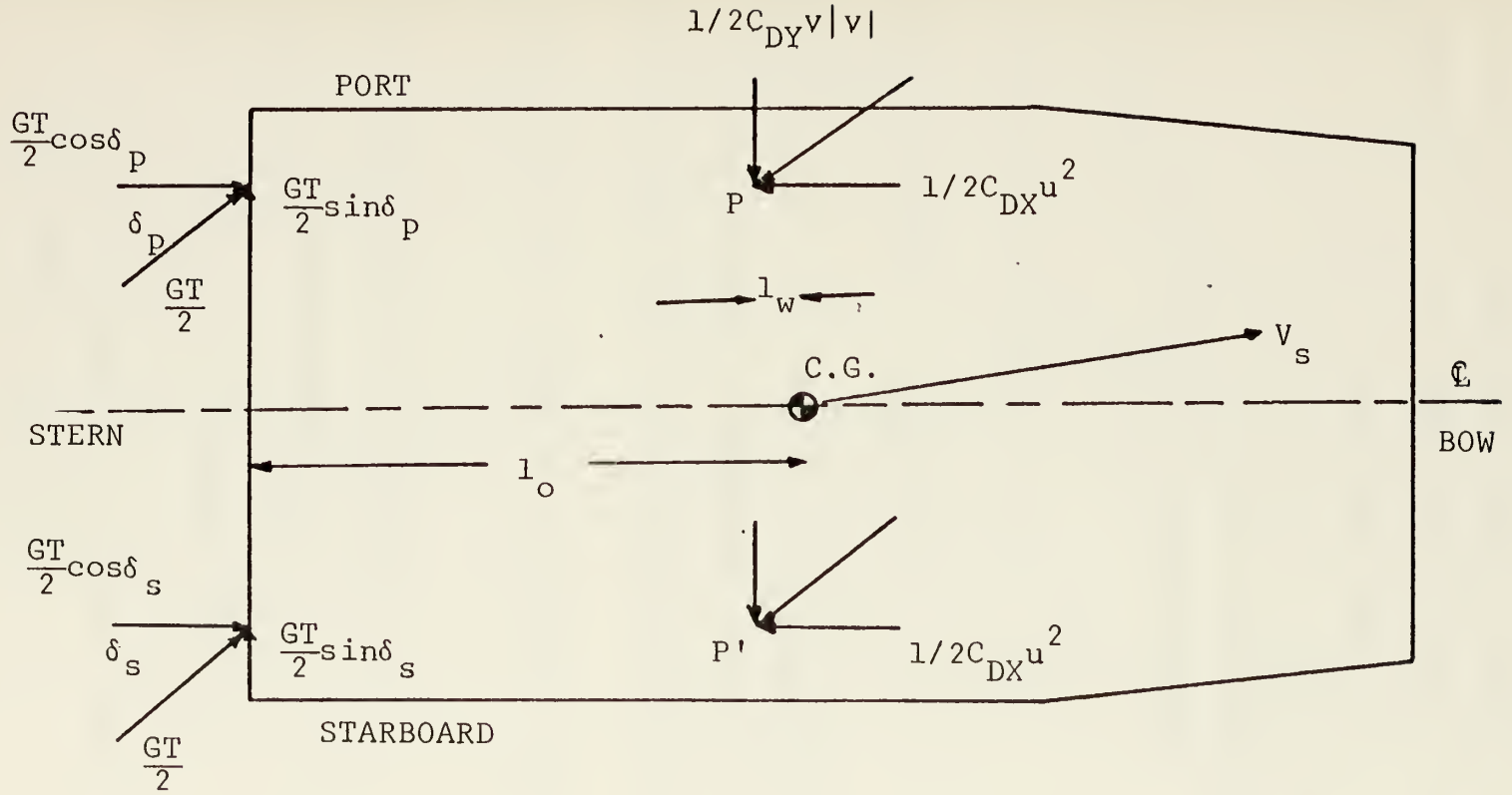


NOTE: $\delta_p = \delta_s = \delta$

Fig. 2 - Forces Acting For A Right Turn

effects. The bubble drag is not included in the initial model.

In like manner, the coefficient $C_{DY}$ in eqs. (9) and (10) models the cross flow drag effects. Note also that the added mass term has been temporarily omitted and will be added later, especially in the 3KSES study since its contribution to the XR-3 model is almost nonexistent [Ref. 6].

Substitution of equations (8), (9) and (10) into the equations (1), (2) and (3) provides the basic equations of motion for the three-degrees-of-freedom model:

$$\dot{u} = \frac{1}{m}(GT\cos\delta - C_{DX}u^2) + vr \tag{11}$$

$$\dot{v} = \frac{1}{m}(GT\sin\delta - C_{DY}v|v|) - ur \tag{12}$$

$$\dot{r} = \frac{1}{I_z}(-(GT\sin\delta)l_o + C_{DY}v|v|l_w) \tag{13}$$

Equations (11), (12) and (13) are applicable to any SES craft. Only the particular parameter values to be used in the equations would depend on the particular craft (XR-3 or 3KSES).

In the case of the 3KSES, the equations take the form (see Fig. 3):

$$\dot{u} = \frac{1}{m}(-C_{DX}u^2+(T7+T8+T9+T10)\cos\delta) + vr$$

$$\dot{v} = \frac{1}{m}((T7+T8+T9+T10)\sin\delta - C_{DY}v|v|) - ur$$

$$\dot{r} = \frac{1}{I_z}(C_{DY}(ww)v|v| + [T7\cos\delta S_4 + T8\cos\delta S_3$$

$$- T9\cos\delta S_1 - T10\cos\delta S_2 - (T7\sin\delta + T8\sin\delta + T9\sin\delta$$

$$+ T10\sin\delta)(OO)] + A_{22}uv(ww))$$

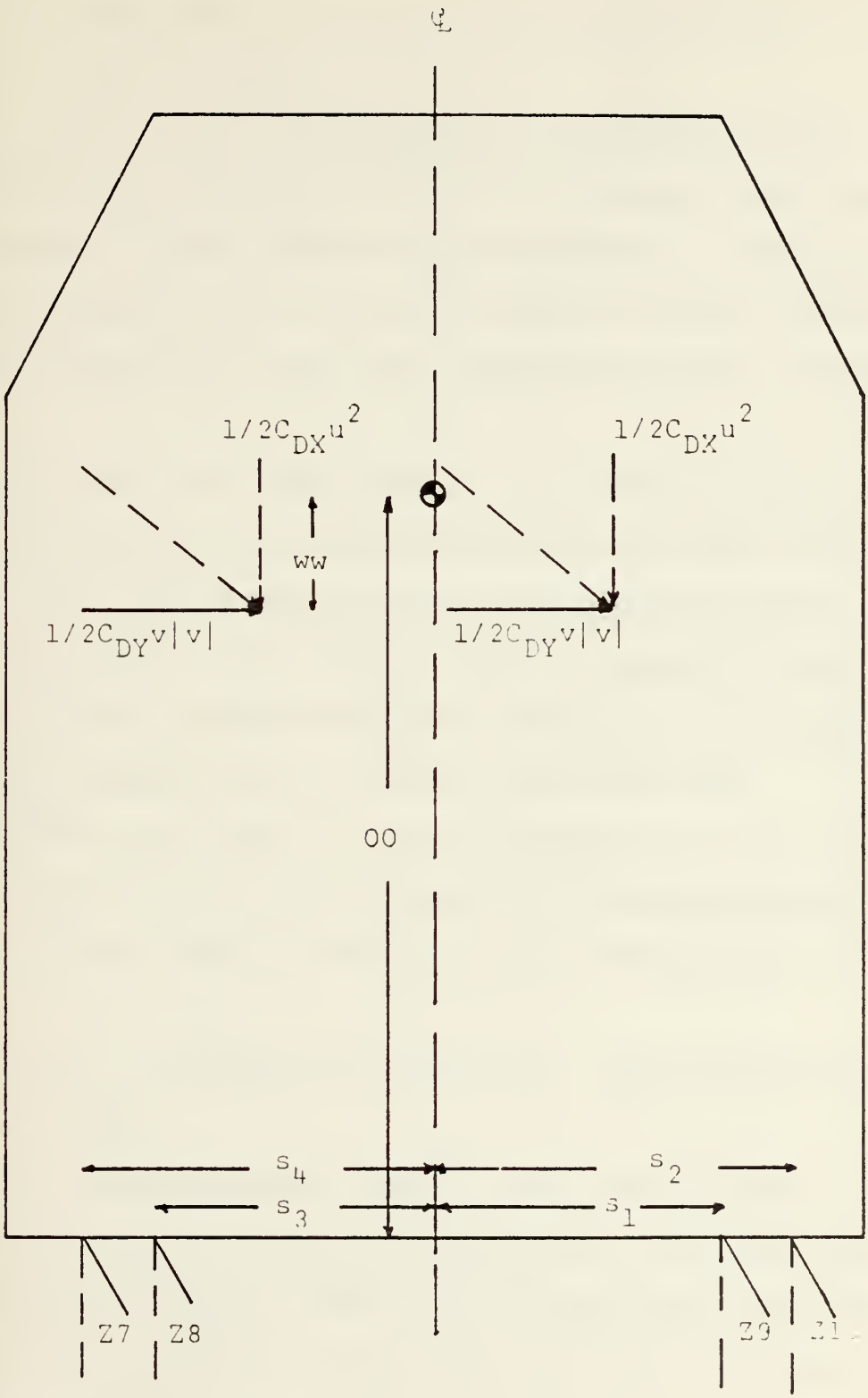


Fig. 3 - Forces Acting On The 4000 Ton Craft For A Right Turn

$\dot{\psi} = r$

$\dot{x}_o = u\cos\psi - v\sin\psi$

$\dot{y}_o = u\sin\psi + v\cos\psi$

For the purpose of this study the thruster's angle $\delta$ was the same for all thrusters except the starboard one, which in the case of thrust failure was considered 0° (thruster oriented straight ahead) and in the case of thrust reversal it was considered as being 180° (thruster oriented straight astern).

In the first case, the thrust of the failed thruster was set to zero pounds and in the second case the thrust was set to full value (98000 pounds for 56 Kts operation speed). That means that either in the case of thrust failure or thrust reversal of the starboard thruster, the rest of the thrusters are ganged together and act in the same direction.

Therefore, the angle $\delta$ can be redefined as Z7, Z8, Z9 and Z10 as shown in Fig. 3 to correspond to the appropriate thrusters and in both cases Z7=Z8=Z9 with Z10 being either 0 or $\pi$ radians.

In order to linearize the equations, the following assumptions were made:

1. The maximum rudder angle is less than or equal to 30 degrees and for most high speed manueuvers the rudder angle stays below 15 degrees. Thus, by letting $\cos\delta \approx 1$ and $\sin\delta \approx \delta$ (where $\delta$ is in radians), the difference from the actual values for $\delta = .2618$ rads = 15° is

a. $\cos 15^\circ = .966$, difference $= \frac{1-.966}{.966} \times 100\% = 3.5\%$

b. $\sin 15^\circ = .2588$, difference $= \frac{.2618-.2588}{.2588}$

$\times 100\% = 1.15\%$

Differences with these magnitudes should not introduce large deviations from the linear design when applied to the nonlinear equations. Thus in the analysis $\delta_{max}$ was restricted to 15 degrees or if $\delta_{max}$ exceeds 15 degrees it probably will be of short duration and will then not introduce large errors in the design values for control.

2. The yaw angle $\psi$ was considered to be less than 10 degrees which agrees very well with the results obtained from the simulation of the craft.

3. Even though the sign of the sway velocity changes depending on the particular situation occuring, the term $v|v|$ was considered as $v^2$.

With the above assumptions, the equations for the 3KSES become:

$$f_1 = \dot{u} \approx \frac{1}{m} (-C_{DX}u^2+T7+T8+T9+T10) + vr$$

$$f_2 = \dot{v} \approx \frac{1}{m} ((T7+T8+T9+T10)\delta - C_{DY}v^2) - ur$$

$$f_3 = \dot{r} \approx \frac{1}{I_z} (C_{DY}v^2(ww)+T7S_4+T8S_3-T9S_1$$

$$- T10S_2-(T7+T8+T9+T10)\delta(OO)+A_{22}uv(ww))$$

$$f_4 = \dot{\psi} = r$$

$$f_5 = \dot{x}_o \approx u-v\psi$$

$$f_6 = \dot{y}_o \approx u\psi + v$$

Defining the state variables

$$x_1 \triangleq u - u_o$$

$$x_2 \triangleq v - v_o$$

$$x_3 \triangleq r - r_o$$

$$x_4 \triangleq \psi - \psi_o$$

$$x_5 \triangleq x_o - x_{oo}$$

$$x_6 \triangleq y_o - y_{oo}$$

$$\mu_1 \triangleq T7 - T7_o$$

$$\mu_2 \triangleq Z7 - Z7_o$$

Then, $\dot{x}_1 = \dot{u}$

$$\dot{x}_2 = \dot{v}$$

$$\dot{x}_3 = \dot{r}$$

$$\dot{x}_4 = \dot{\psi}$$

$$\dot{x}_5 = \dot{x}_o$$

$$\dot{x}_6 = \dot{y}_o$$

The linear state equation coefficients are:

$$\frac{\partial f_1}{\partial u} = \left.\frac{-2C_{DX}u}{m}\right|_{u=u_o} = \frac{-2C_{DX}u_o}{m}$$

$$\frac{\partial f_1}{\partial v} = r\Big|_{r=r_o} = r_o$$

$$\frac{\partial f_1}{\partial r} = v\Big|_{v=v_o} = v_o$$

$$\frac{\partial f_1}{\partial \psi} = \frac{\partial f_1}{\partial x_o} = \frac{\partial f_1}{\partial y_o} = 0$$

$$\frac{\partial f_1}{\partial T7} = \frac{1}{m}$$

$$\frac{\partial f_1}{\partial Z7} = 0$$

$$\frac{\partial f_2}{\partial u} = -r\Big|_{r=r_o} = -r_o$$

$$\frac{\partial f_2}{\partial v} = \frac{-2C_{DY}v}{m}\Bigg|_{v=v_o} = \frac{-2C_{DY}v_o}{m}$$

$$\frac{\partial f_2}{\partial r} = -u\Big|_{u=u_o} = -u_o$$

$$\frac{\partial f_2}{\partial \psi} = \frac{\partial f_2}{\partial x_o} = \frac{\partial f_2}{\partial y_o} = 0$$

$$\frac{\partial f_2}{\partial T7} = \frac{Z7}{m}\Big|_{Z7=Z7_o} = \frac{Z7_o}{m}$$

$$\frac{\partial f_2}{\partial Z7} = \frac{T7+T8+T9}{m}\Bigg|_{\substack{T7=T7_o \\ T8=T8 \\ T9=T9}} = \frac{T7_o+T8+T9}{m}$$

$$\frac{\partial f_3}{\partial u} = \frac{A_{22}v(ww)}{I_z}\Bigg|_{v=v_o} = \frac{A_{22}v_o(ww)}{I_z}$$

$$\frac{\partial f_3}{\partial v} = \frac{2C_{DY}v(ww)+A_{22}u(ww)}{I_z}\Bigg|_{\substack{u=u_o \\ v=v_o}} = \frac{(2C_{DY}v_o+A_{22}u_o)(ww)}{I_z}$$

$$\frac{\partial f_3}{\partial r} = \frac{\partial f_3}{\partial \psi} = \frac{\partial f_3}{\partial x_o} = \frac{\partial f_3}{\partial y_o} = 0$$

$$\frac{\partial f_3}{\partial T7} = \frac{S_4-Z7(00)}{I_z}\Bigg|_{Z7=Z7_o} = \frac{S_4-Z7_o(00)}{I_z}$$

$$\frac{\partial f_3}{\partial Z7} = \frac{-(00)(Z7+Z8+Z9)}{I_z}\Bigg|_{Z7=Z7_o} = \frac{-(00)(Z7_o+Z8+Z9)}{I_z}$$

$$\frac{\partial f_4}{\partial u} = \frac{\partial f_4}{v} = \frac{\partial f_4}{\partial \psi} = \frac{\partial f_4}{\partial x_o} = \frac{\partial f_4}{\partial y_o} = \frac{\partial f_4}{\partial T7} = \frac{\partial f_4}{\partial Z7} = 0$$

$$\frac{\partial f_4}{\partial r} = 1$$

$$\frac{\partial f_5}{\partial u} = 1$$

$$\frac{\partial f_5}{\partial v} = -\psi\Big|_{\psi=\psi_o} = -\psi_o$$

$$\frac{\partial f_5}{\partial \psi} = -v\Big|_{v=v_o} = -v_o$$

$$\frac{\partial f_5}{\partial x_o} = \frac{\partial f_5}{\partial r} = \frac{\partial f_5}{\partial y_o} = \frac{\partial f_5}{\partial T7} = \frac{\partial f_5}{\partial Z7} = 0$$

$$\frac{\partial f_6}{\partial u} = \psi\Big|_{\psi=\psi_o} = \psi_o$$

$$\frac{\partial f_6}{\partial v} = 1$$

$$\frac{\partial f_6}{\partial \psi} = u\Big|_{u=u_o} = u_o$$

$$\frac{\partial f_6}{\partial r} = \frac{\partial f_6}{\partial x_o} = \frac{\partial f_6}{\partial y_o} = \frac{\partial f_6}{\partial T7} = \frac{\partial f_6}{\partial Z7} = 0$$

In standard form the system becomes:

$\dot{\underset{\sim}{x}} = \underset{\sim\sim}{A}\underset{\sim}{x} + \underset{\sim x}{B}\underset{\sim}{\mu}$ where

$$\underset{\sim}{\dot{x}} = \begin{bmatrix} \dot{x}_1 \\ \dot{x}_2 \\ \dot{x}_3 \\ \dot{x}_4 \\ \dot{x}_5 \\ \dot{x}_6 \end{bmatrix} \qquad \underset{\sim}{\mu} = \begin{bmatrix} \Delta T7 \\ \\ \Delta Z7 \end{bmatrix}$$

$$\underset{\sim}{A} = \begin{bmatrix} a_{11} & a_{12} & a_{13} & 0 & 0 & 0 \\ a_{21} & a_{22} & a_{23} & 0 & 0 & 0 \\ a_{31} & a_{32} & 0 & 0 & 0 & 0 \\ 0 & 0 & a_{43} & 0 & 0 & 0 \\ a_{51} & a_{52} & 0 & a_{54} & 0 & 0 \\ a_{61} & a_{62} & 0 & a_{64} & 0 & 0 \end{bmatrix}$$

$$\underset{\sim}{B} = \begin{bmatrix} b_{11} & 0 \\ b_{21} & b_{22} \\ b_{31} & b_{32} \\ 0 & 0 \\ 0 & 0 \\ 0 & 0 \end{bmatrix}$$

and

$$a_{11} = \frac{-2C_{DX}u_o}{m}$$

$$a_{12} = r_o$$

$$a_{13} = v_o$$

$$a_{21} = -r_o$$

$$a_{22} = -\frac{2C_{DY}v_o}{m}$$

$$a_{23} = -u_o$$

$$a_{31} = \frac{A_{22}v_o(ww)}{I_z}$$

$$a_{32} = \frac{(2C_{DY}v_o+A_{22}u_o)(ww)}{I_z}$$

$$a_{43} = 1$$

$$a_{51} = 1$$

$$a_{52} = -\psi_o$$

$$a_{54} = -v_o$$

$$a_{61} = \psi_o$$

$$a_{62} = 1$$

$$a_{64} = u_o$$

$$b_{11} = \frac{1}{m}$$

$$b_{21} = \frac{Z7_o}{m}$$

$$b_{22} = \frac{T7_o+T8+T9}{m}$$

$$b_{31} = \frac{S_4-Z7_o(00)}{I_z}$$

$$b_{32} = \frac{-(00)(T7_o+T8+T9)}{I_z}$$

So, by linearizing around the equilibrium point ($u_o$, $v_o$, $r_o$, $\psi_o$, $x_{oo}$, $y_{oo}$) the equations become:

$$\dot{x}_1 = \frac{-2C_{DX}u_o}{m} x_1 + r_o x_2 + v_o x_3 + \frac{1}{m} C_1$$

$$\dot{x}_2 = -r_o x_1 - \frac{2C_{DY}v_o}{m} x_2 - u_o x_3 + \frac{Z7_o}{m} C_1$$

$$+ \left(\frac{T7_o+T8+T9}{m}\right) C_2$$

$$\dot{x}_3 = \frac{A_{22}v_o(ww)}{I_z} x_1 + \frac{(2C_{DY}v_o+A_{22}u_o)(ww)}{I_z} x_2$$

$$+ \left(\frac{S_4-Z7_o(00)}{I_z}\right) C_1 - \frac{(00)(T7_o+T8+T9)}{I_z} C_2$$

$$\dot{x}_4 = x_3$$

$$\dot{x}_5 = x_1 - \psi_o x_2 - v_o x_4$$

$$\dot{x}_6 = \psi_o x_1 + x_2 + u_o x_4$$

The above equations were used to determine by computer simulation the required gains for the state feedbacks using the linear regulator solution [Refs. 7, 8 and 9].

In order to obtain the equilibrium point, the nonlinear equations were used by setting $\dot{u}=0$, $\dot{v}=0$, $\dot{r}=0$ and determining, after a failure had occured and the system being corrected as far as was possible by the trial and error algorithm (see Chapter III), the "steady state" values for the above mentioned variables.

Two "steady state" runs were made, one with the starboard thruster failed and the other with the starboard thruster reversed.

The "steady state" values obtained are listed in Tables I and II.

TABLE I

Steady State Values (Thruster Failure)

| Surge Velocity (ft/s) | Sway Velocity (ft/s) | Angular Velocity (rad/s) | Yaw Angle (rad) | Track Deviation (ft) |
|---|---|---|---|---|
| 74.422 | 1.86 | $-.7415 \times 10^{-7}$ | -.0254 | 10.88 |

| Port Thrust (lbf) |
|---|
| 87600 |

TABLE II

Steady State Values (Thruster Reversal)

| Surge Velocity | Sway Velocity | Angular Velocity | Yaw Angle | Track Deviation |
|---|---|---|---|---|
| (ft/s) | (ft/s) | (rad/s) | (rad) | (ft) |
| 55.66 | 2.62 | $-.3417 \times 10^{-5}$ | -.04709 | 21.41 |

For this study, the steady state value achieved by the simulation with the thrust failure were used for the development of the linear system and the subsequent use of the optimal control scheme. The choice was quite arbitrary but, nevertheless, the results show that the system does behave well, no matter which one of the two emergencies (thrust failure or thrust reversal) occurs.

## III. TRIAL AND ERROR DESIGN

### A. INTRODUCTION

Taking into account the impressive speed of the surface effect ship, it is evident that there is a need for controlling it either during straight runs or during an emergency which would be manifested by the loss of thrust of one thruster or even by the thrust reversal.

As was seen from the results of computer runs with the model, the behavior of the ship during a failure was predictable but nevertheless disturbing because the ship veered quite rapidly from the track that it was following before the failure.

Therefore, the goal of the control procedure was twofold. First, it was required to maintain control of the ship and second to maintain that control in some acceptable manner.

### B. ANALYSIS

As was evidenced (see Fig. 4), when the outer starboard thruster experienced a complete thruster failure, the ship, without any corrective action with respect to nozzle movement or thrust variation of the remaining jet nozzles, veered to the right and actually entered a turn.

By analyzing this behavior, it was seen that the parameters changing the most were the yaw angle $\psi$ and the deflection from the original track which was assumed straight ahead.

Intuitively then, it was evident that from the available variables, $\psi$ and $y_o$ would be most eligible to control in order to bring the ship back or close to the original track. Because it was quite clear that, if the heading (yaw angle) was minimized as well as the deviation from the track, the ship would follow again the original track or a track that was parallel to that one.

Therefore, the corrective action chosen was nozzle deflection as a function of the yaw angle and the deviation from the original track.

Furthermore, since positive nozzle angle drives the ship to the left, by selecting deviation to the right as being positive and yaw angle to the right being positive to the right, it was quite clear that the nozzle action would only involve $\psi$ and $y_o$ without any sign change.

Thus, the problem reduced to the point of determining the appropriate gains for $\psi$ and $y_o$ and the rudder action took the form $z=K_1\psi+K_2y_o$.

## C. TRIAL AND ERROR PROCEDURE

As a beginning, $K_1$ was arbitrarily selected to be 1000 and $K_2$ being 5. It was seen that the action of the rudder was too heavy and the movement of the ship was quite erratic and at the end became unbounded.

Therefore, both gains were decreased to $K_1=8$ and $K_2=.035$, which gave a more acceptable performance (Fig. 14).

The thus established rudder algorithm proved to be adequate even when a reversal failure of the starboard thruster was inflicted (Fig. 21).

As a further improvement, the idea of modulating the thrust of the left thruster during a failure was brought into effect. That is, the thrust was varied to smaller values by the amount of the deflection of the ship off the original track (Fig. 20).

The above scheme was used for all the runs presented in Figs. 14 through 27.

In order to evaluate all the above corrective actions, the performance indices described in Chapter IV were used.

As can be seen, the ship actually moves down the track with a large drift angle. That is, although a corrective rudder action is maintained, the ship does not turn into a circle and also it does not veer to the left or to the right although there exists a sway velocity and asymmetrical thrust.

# IV. LINEAR REGULATOR DESIGN

## A. INTRODUCTION

The theory behind the linear regulator is well established and need not be repeated here. For a brief discussion, see Appendix A.

After the linearization of the system's equations around an equilibrium point, the IBM/360 was used to obtain the solution of the matrix Riccati equation, using the method presented in [Refs. 8 and 9].

## B. ANALYSIS

It was evident that in order to achieve a parallel track for the craft after a failure had occured, the deflection from the original track should come into play. Also, in order for the craft to maintain this parallel track, the yaw angle should be minimized as well as the angular velocity about the z axis.

As with the trial and error procedure the corrective action chosen was ganged deflection of the operating nozzles and thrust control of the port thruster to compensate for the failed starboard thruster.

## C. PERFORMANCE INDICES

One of the basic problems of modern control theory is the translation of system specifications, often in such

subjective terms as "good rise time with reasonable overshoot", into the form of a performance index. Furthermore, after the selection of a performance index, the designer has to make an initial guess for the weighting of the state variables and adjust them after comparing time histories of the controlled system.

For the purpose of this study, the following performance index was selected:

$$J = \int_0^{t_f} (\underset{\sim}{x}^T \underset{\sim\sim}{Q} \underset{\sim}{x} + \underset{\sim}{\mu}^T \underset{\sim\sim}{R} \underset{\sim}{\mu}) \, dt$$

Concerning the weighting of the variables, considerable experimentation was done. In the final form of the above performance index the weighting matrices $\underset{\sim}{Q}$ and $\underset{\sim}{R}$ were:

$$\underset{\sim}{Q} = \begin{bmatrix} 0 & 0 & 0 & 0 & 0 & 0 \\ 0 & 0 & 0 & 0 & 0 & 0 \\ 0 & 0 & 20000 & 0 & 0 & 0 \\ 0 & 0 & 0 & 8 & 0 & 0 \\ 0 & 0 & 0 & 0 & 0 & 0 \\ 0 & 0 & 0 & 0 & 0 & .035 \end{bmatrix}$$

$$\underset{\sim}{R} = \begin{bmatrix} 1 & 0 \\ 0 & 1 \end{bmatrix}$$

The final weights used reflect the importance given to the yaw angle, the angular velocity about the z axis and the craft deviation from the original track.

The optimal control inputs obtained are:

$$\underset{\sim}{u}^* = \begin{bmatrix} 0 & 0 & -.00046 & -.0007 & 0 & 0 \\ -.0316 & .684 & 185.7 & 110.7 & 0 & .186 \end{bmatrix} \underset{\sim}{x}$$

The response of the nonlinear system with the above feedback is shown in Figs. 28 through 41.

In order to compare the performance of the craft under the trial and error algorithm, the optimal algorithm and the real time simulation, the following two additional performance indices were used:

$$J_1 = \int_o^{t_f} y_o^2 dt \quad \text{and} \quad J_2 = \int_o^{t_f} (Z7)^2 dt.$$

## V. COMPARISON OF RESULTS

### A. THRUST FAILURE MODE (OPTIMAL ALGORITHM VS. TRIAL AND ERROR ALGORITHM)

Observation of the sea track ($x_o$ vs. $y_o$) (Figs. 14 and 28) indicates that the trial and error algorithm is much less of the desired control algorithm when compared to the optimal, because it appears that the trial and error algorithm does not react fast enough to stabilize the vehicle whereas the optimal does so immediately. The trial and error algorithm does seek out the steady state value of the track deflection but the comparison of the two tracks is dramatic in showing how much better off is the optimal algorithm in controlling the craft during a thrust failure. It must be kept in mind in making this observation that the trial and error design used in this comparison was not developed to its full capabilities. As stated earlier, the trial and error design was intended only as a means of establishing the linear system design.

From the time history shown in Figs. 14 and 28, the vehicle for the same failure scenario reaches a steady state point with the optimal control in 22 seconds whereas with the trial and error control the steady state point would be reached somewhere around 200 seconds or even greater, due to the lightly damped control system.

As can be seen from Figs. 20 and 35 the port thruster is much more active with the trial and error algorithm. The range of modulation covers about 14000 pounds whereas utilization of the optimal algorithm gives a total thrust modulation of 2 pounds. This does not reflect exactly what happens to the port thruster, because as stated earlier in Chapter II as soon as the failure occurs, the port thrust drops to 90% of its full value.

It should also be noted that the trial and error solution seeks the steady state value of the port thruster obtained by the optimal solution.

Comparing Figs. 18 and 32 it can be seen in Fig. 32 that the forward and side thrust as well as the yaw moment reach a steady state within 10 seconds after the initiation of the thruster failure when the optimal solution is used. Instead, when the trial and error solution is used, the craft as shown in Fig. 18 seeks the same steady state but even at 100 sec after the initiation of the failure it has not stabilized. On the average, the values obtained from both algorithms are approximately the same.

However, it is readily apparent that the trial and error control system has poles close to the $j\omega$-axis and as a result exhibits a response of a lightly damped system whereas the optimal control system responds with much faster time constants, which would indicate that this system has poles at a greater distance from the $j\omega$-axis.

B. THRUST REVERSAL MODE (OPTIMAL ALGORITHM VS. TRIAL AND ERROR ALGORITHM)

All the previous comments that were made for the thrust failure mode also apply to the case of a thrust reversal for the starboard thruster. However, due to the increased severity of the forces acting during the thrust reversal and the greater magnitude of the yaw moment (see Figs. 32 and 39), the optimal control exhibits a slightly longer settling time (Figs. 28 and 35).

During the thrust reversal scenario, the absolute magnitudes of the state variables is larger than those experienced during the thrust failure case.

Comparison between the optimal solution time histories and trial and error solution time histories again confirms the fact that optimal state variable feedback provides a more highly damped system, with steady state values being reached within 20 seconds from the initiation of the failure (see Figs. 36, 38, 39 and 40). The trial and error solution is shown in Figs. 22, 24, 25 and 26 which again exhibits a lightly damped time history which would not be acceptable either from a mechanical or ship's efficiency viewpoint.

It is observed (Fig. 23) that the trial and error solution requires the operational thrusters to be extended to their mechanical limits of +.5 radians even at the time =100 seconds point, whereas the optimal solution in Fig. 37 has a peak value for the thrusters of approximately +.4 radians and never requires them to extend to their mechanical limit.

Fig. 4 - Sea Track, Thruster Failure, No Correction

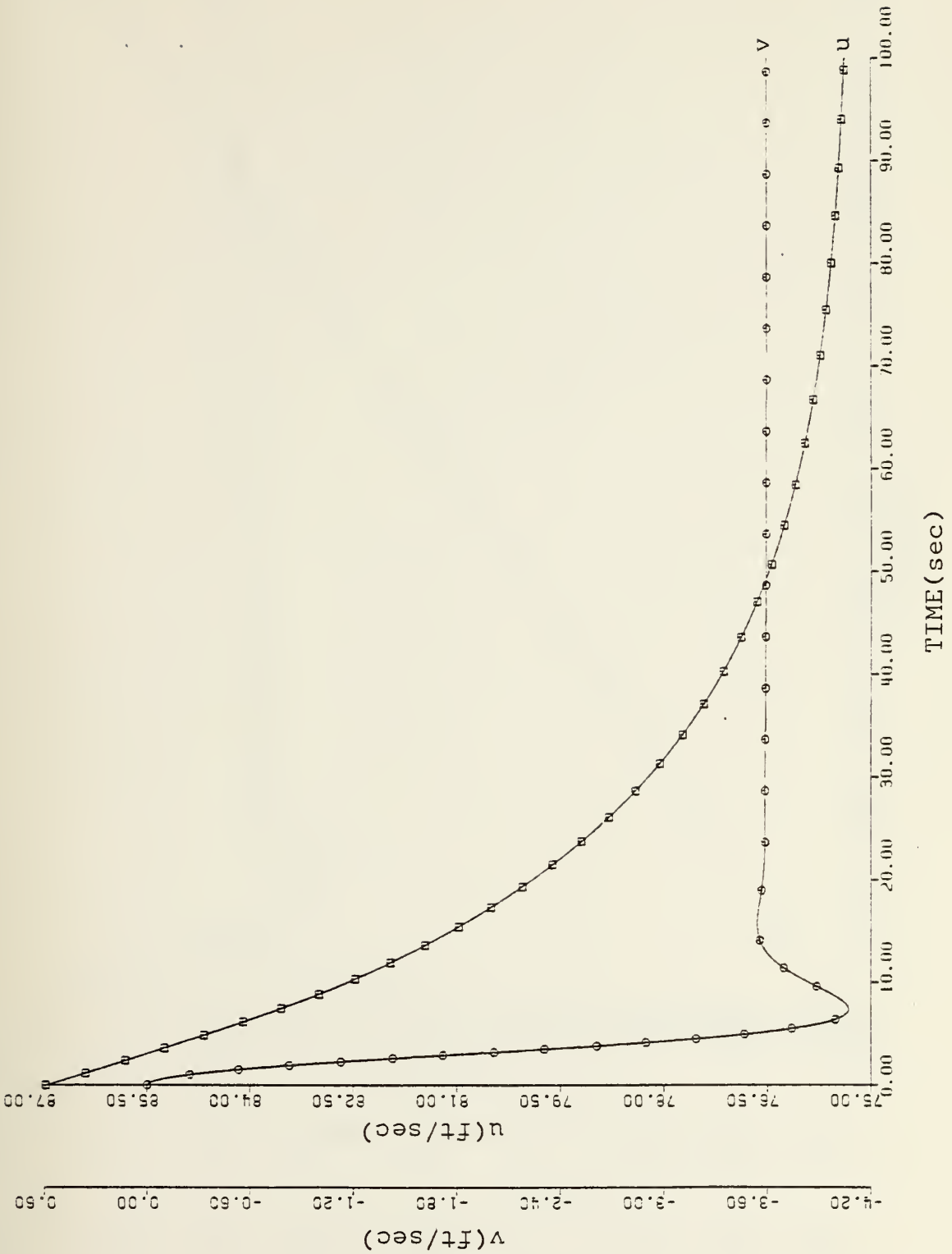


Fig. 5 - Surge and Sway Velocities Vs. Time, Thruster Failure, No Correction

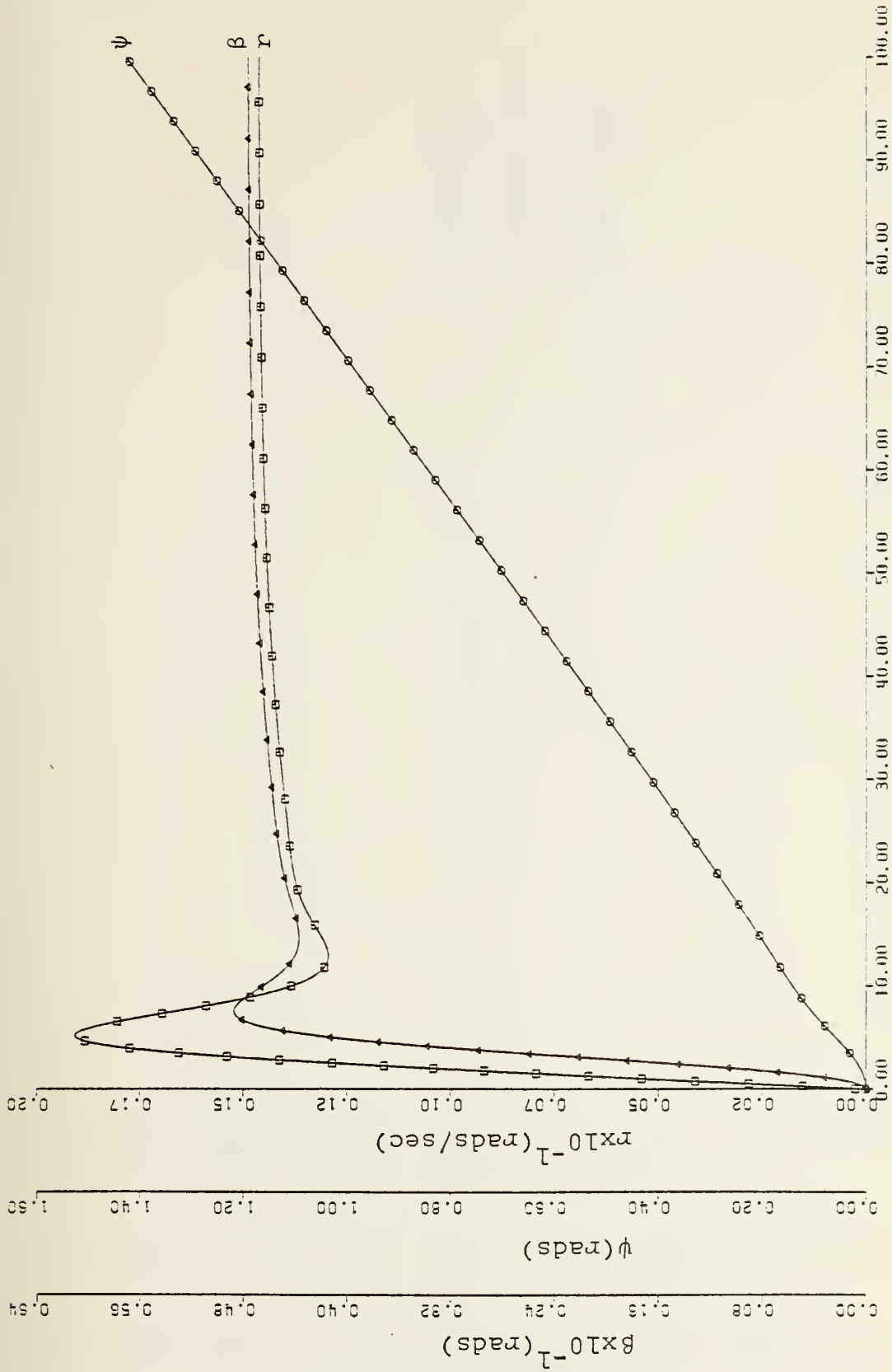


Fig. 6 - Yaw Rate, Heading and Slip Angle Vs. Time, Thruster Failure, No Correction

Fig. 7 - Forward Force, Side Force and Turn Moment Vs. Time, Thruster Failure, No Correction

Fig. 8 - Surge, Sway and Yaw Acceleration Vs. Time, Thruster Failure, No Correction

Fig. 9 - Sea Track, Thruster Reversal, No Correction

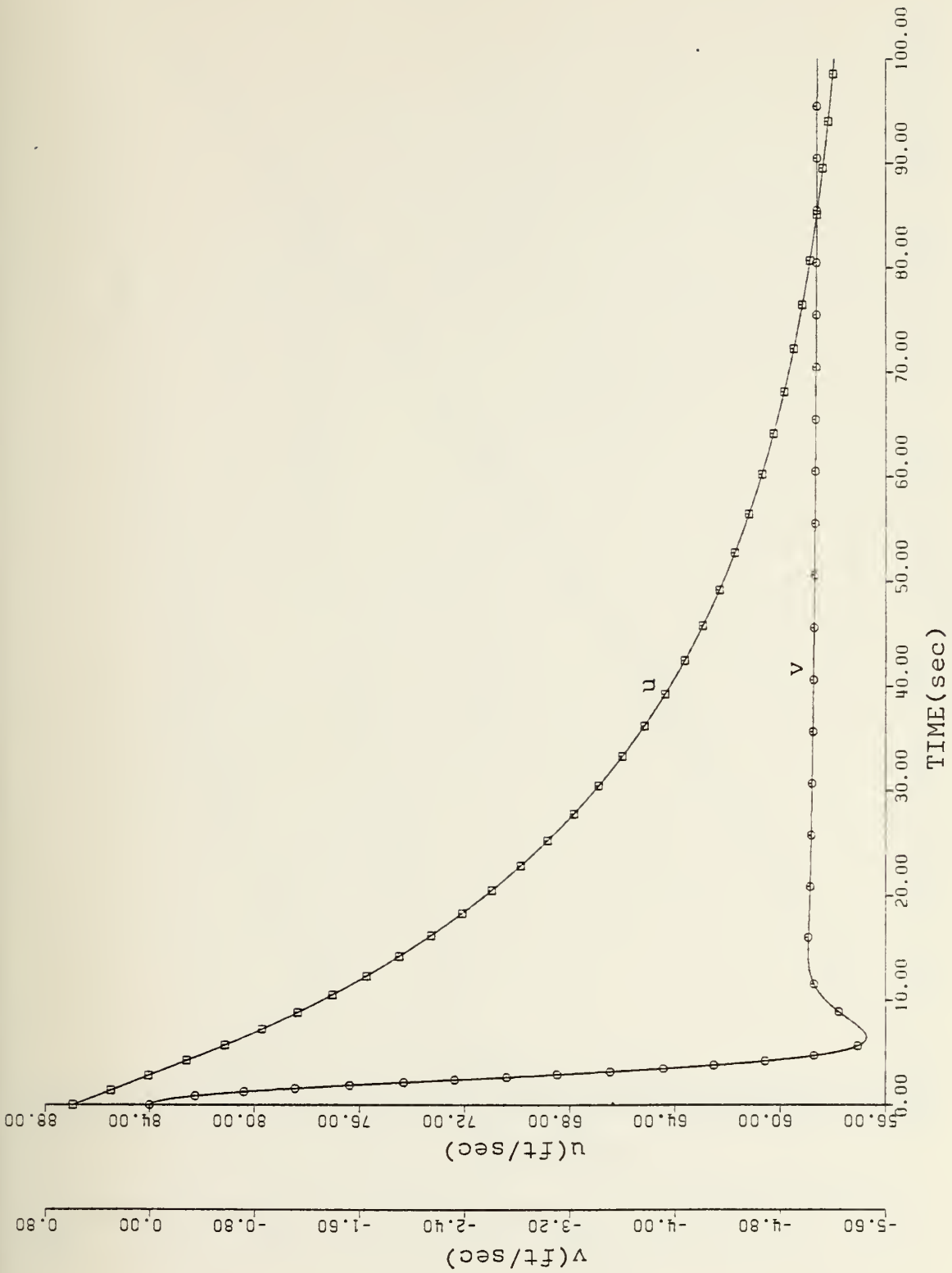


Fig. 10 - Surge and Sway Velocities Vs. Time, Thruster Reversal, No Correction

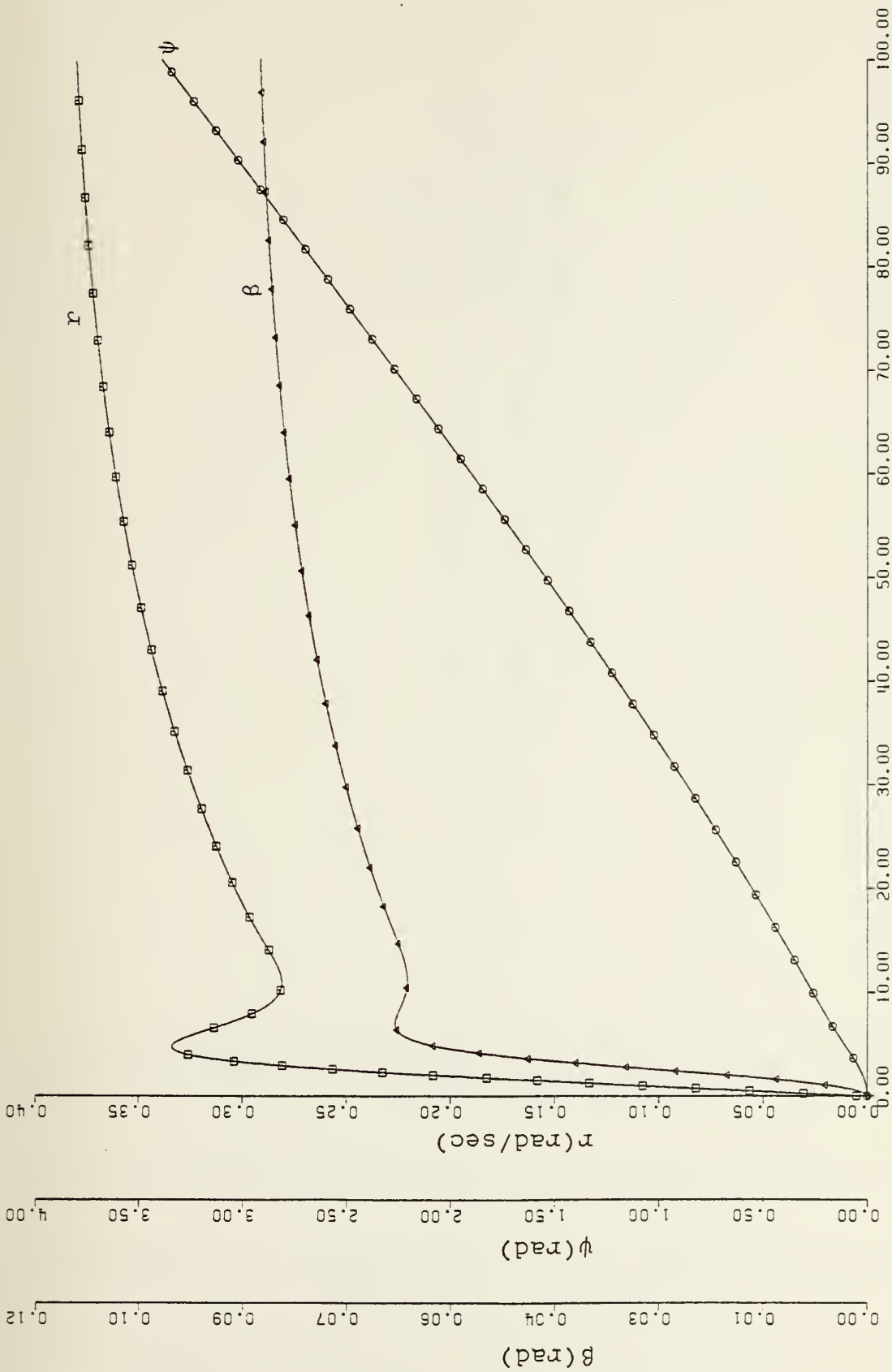


Fig. 11 - Yaw Rate, Heading and Slip Angle Vs. Time, Thruster Reversal, No Correction

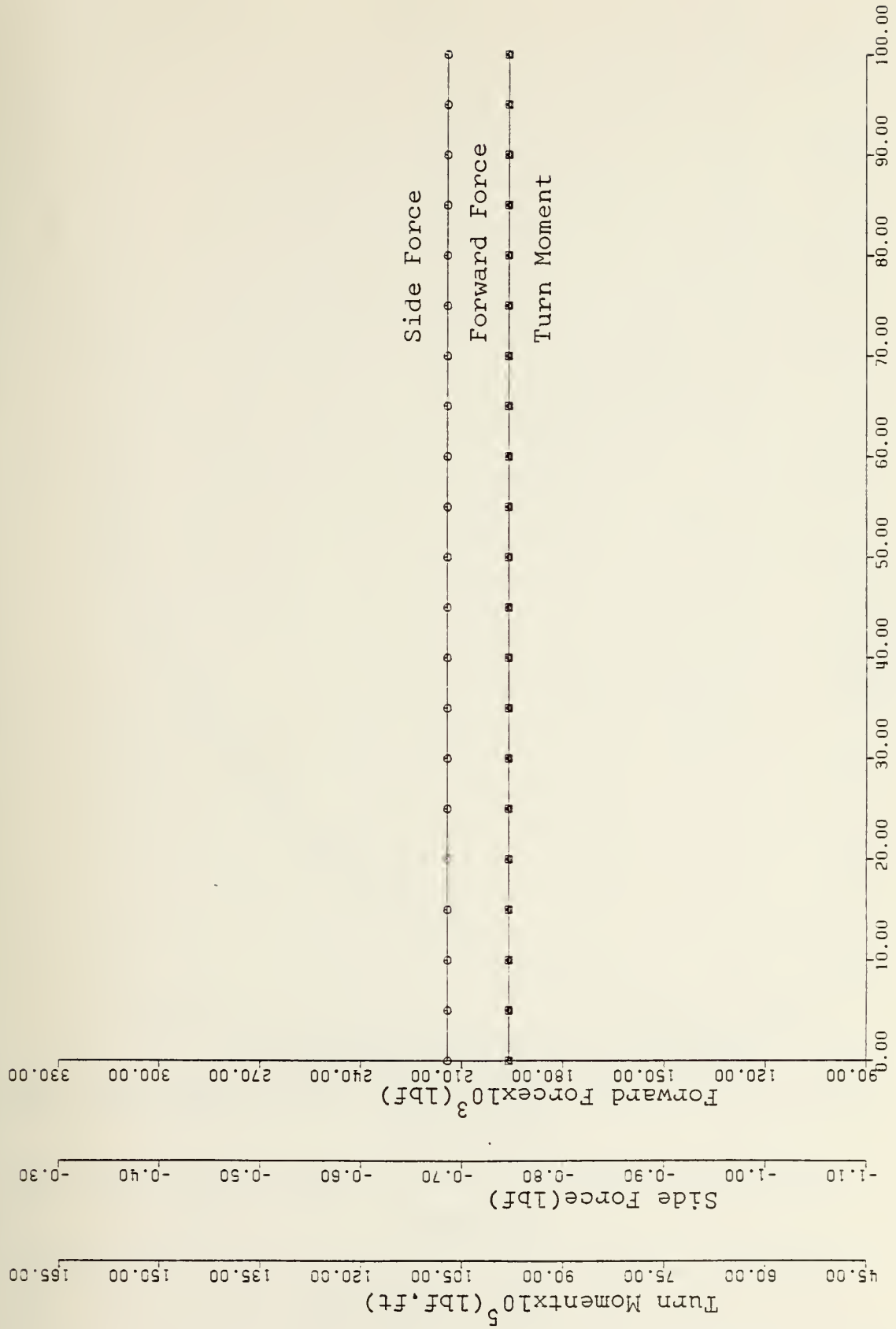


Fig. 12 - Forward Force, Side Force and Turn Moment Vs. Time, Thruster Reversal, No Correction

Fig. 13 - Surge, Sway and Yaw Acceleration, Thruster Reversal, No Correction

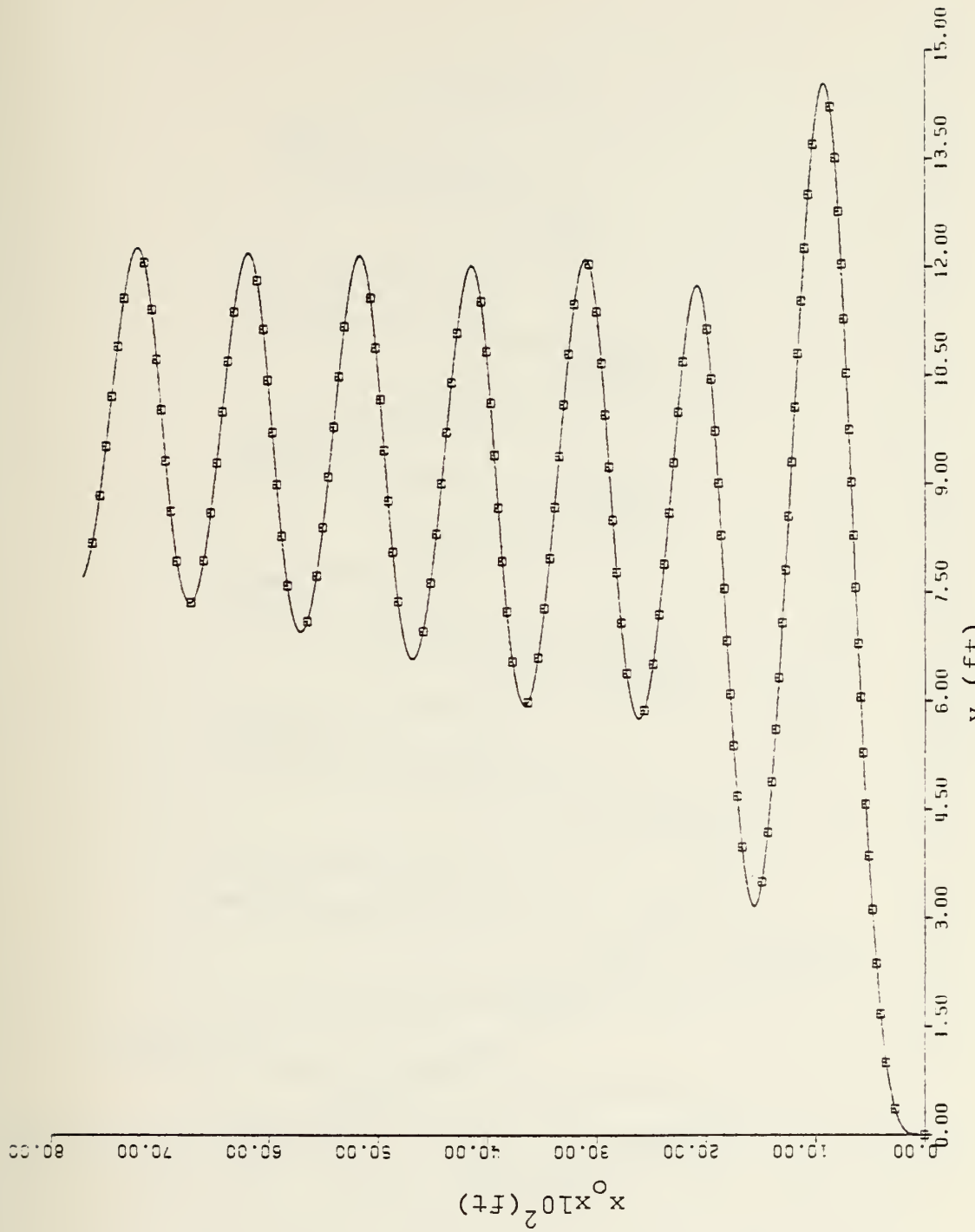


Fig. 14 - Sea Track, Thruster Failure, Trial and Error Solution


Fig. 15 - Surge and Sway Velocities Vs. Time, Thruster Failure, Trial and Error Solution

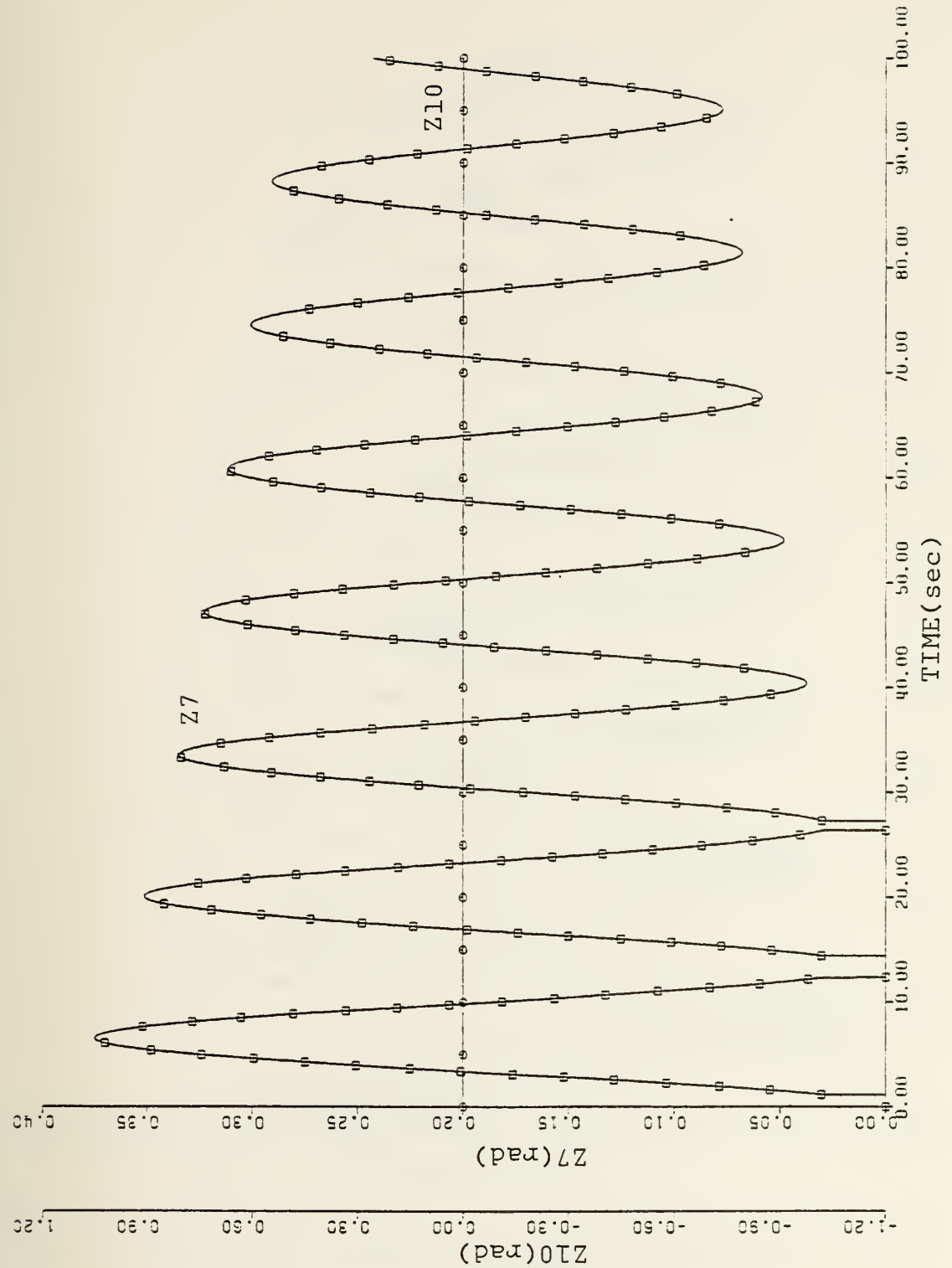


Fig. 16 - Effector Action Vs. Time, Thruster Failure, Trial and Error Solution

Fig. 17 - Yaw Rate, Heading and Slip Angle Vs. Time, Thruster Failure, Trial and Error Solution

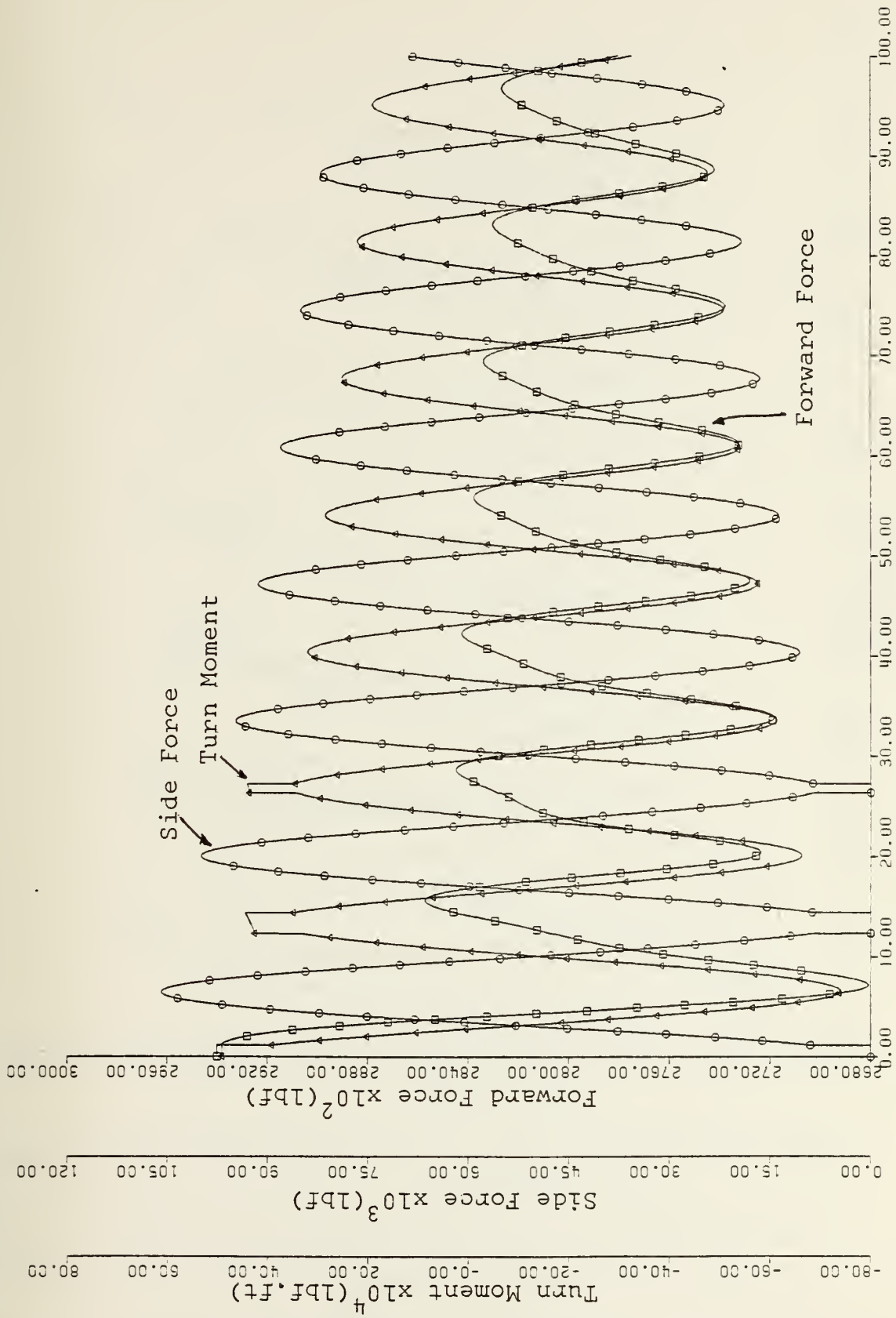


Fig. 18 - Forward Force, Side Force and Turn Moment Vs. Time, Thruster Failure, Trial and Error Solution

Fig. 19 - Surge, Sway and Yaw Acceleration Vs. Time, Thruster Failure, Trial and Error Solution

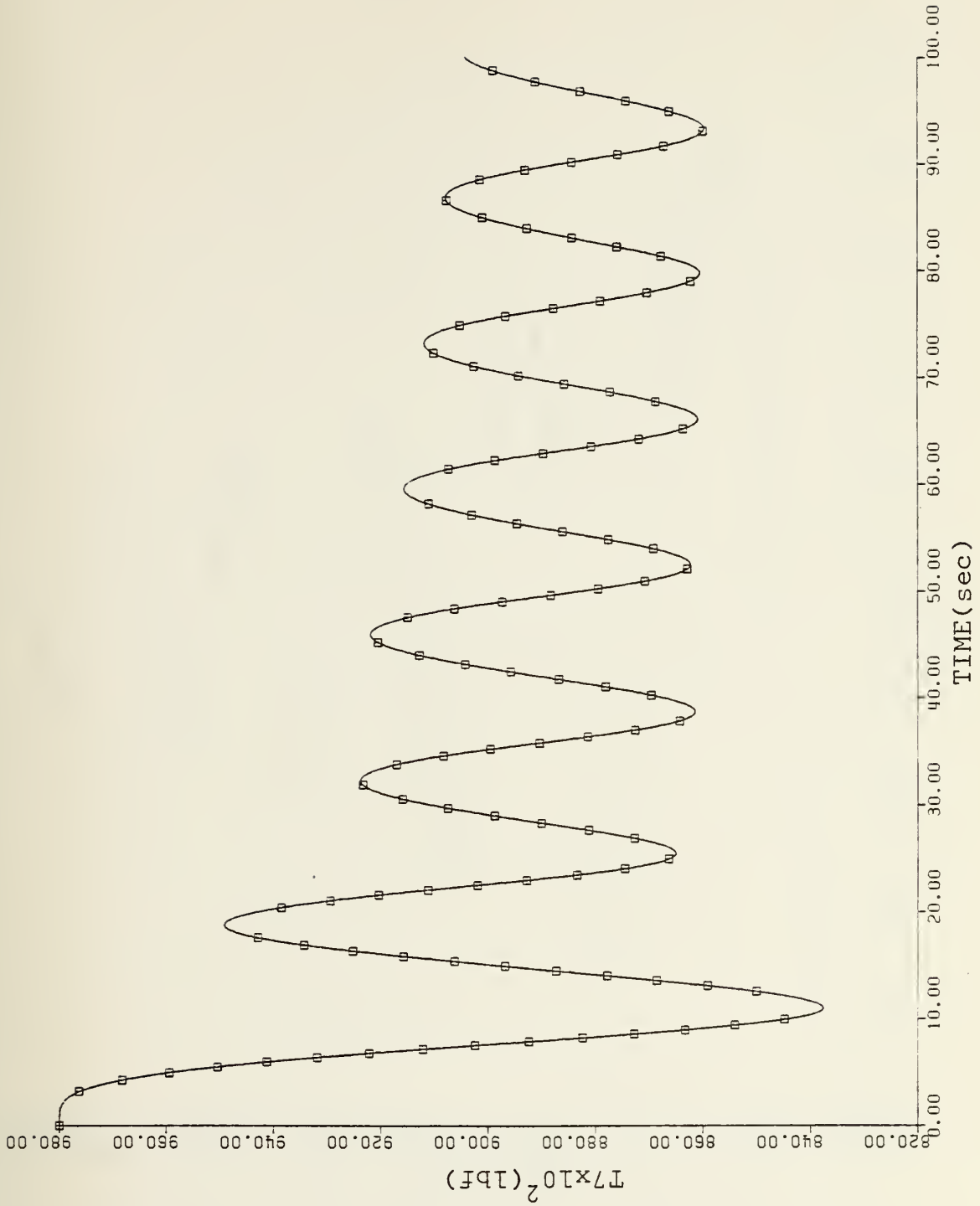


Fig. 20 - Port Thruster Action vs. Time, Thruster Failure, Trial and Error Solution

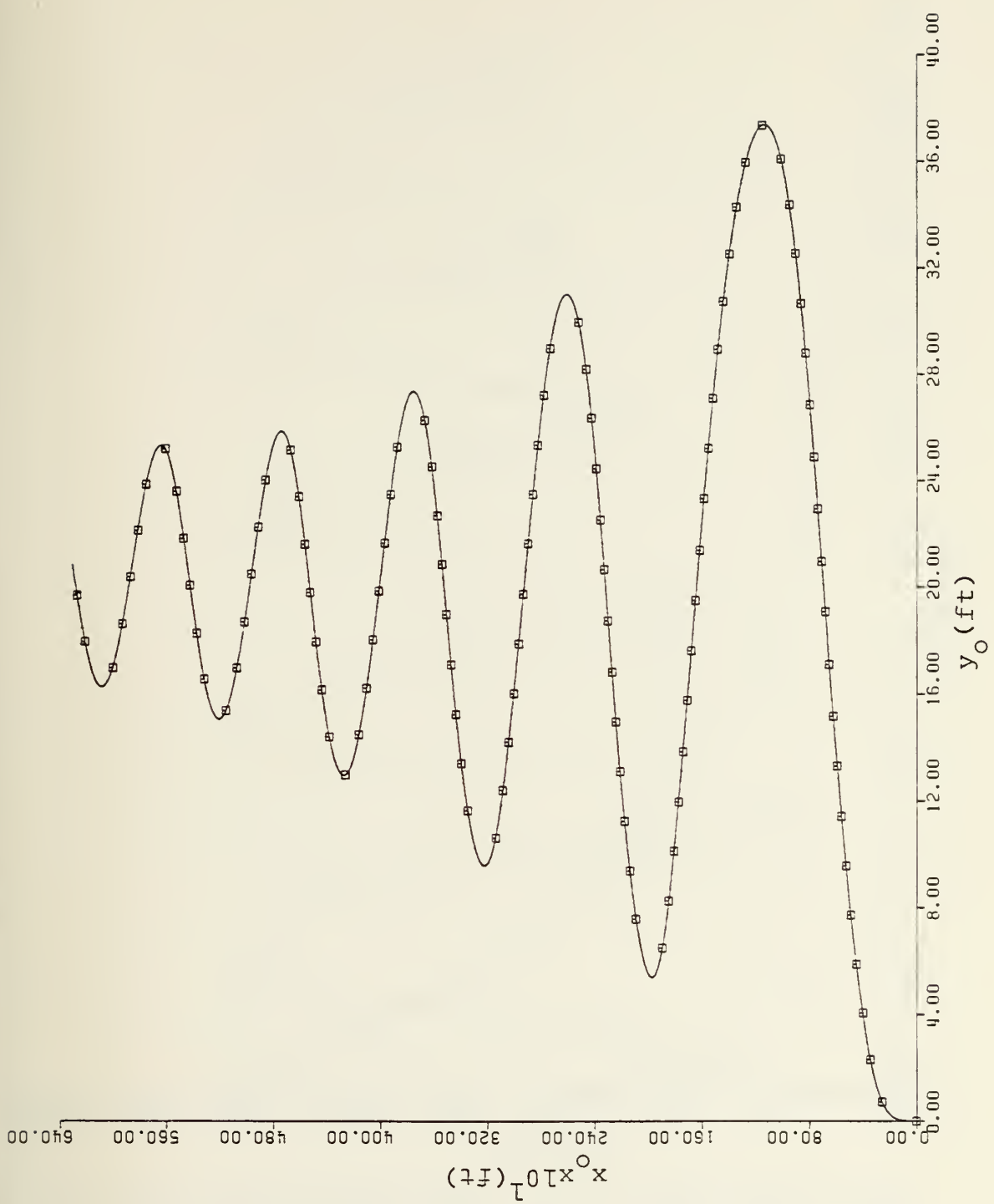


Fig. 21 - Sea Track, Thruster Reversal, Trial and Error Solution

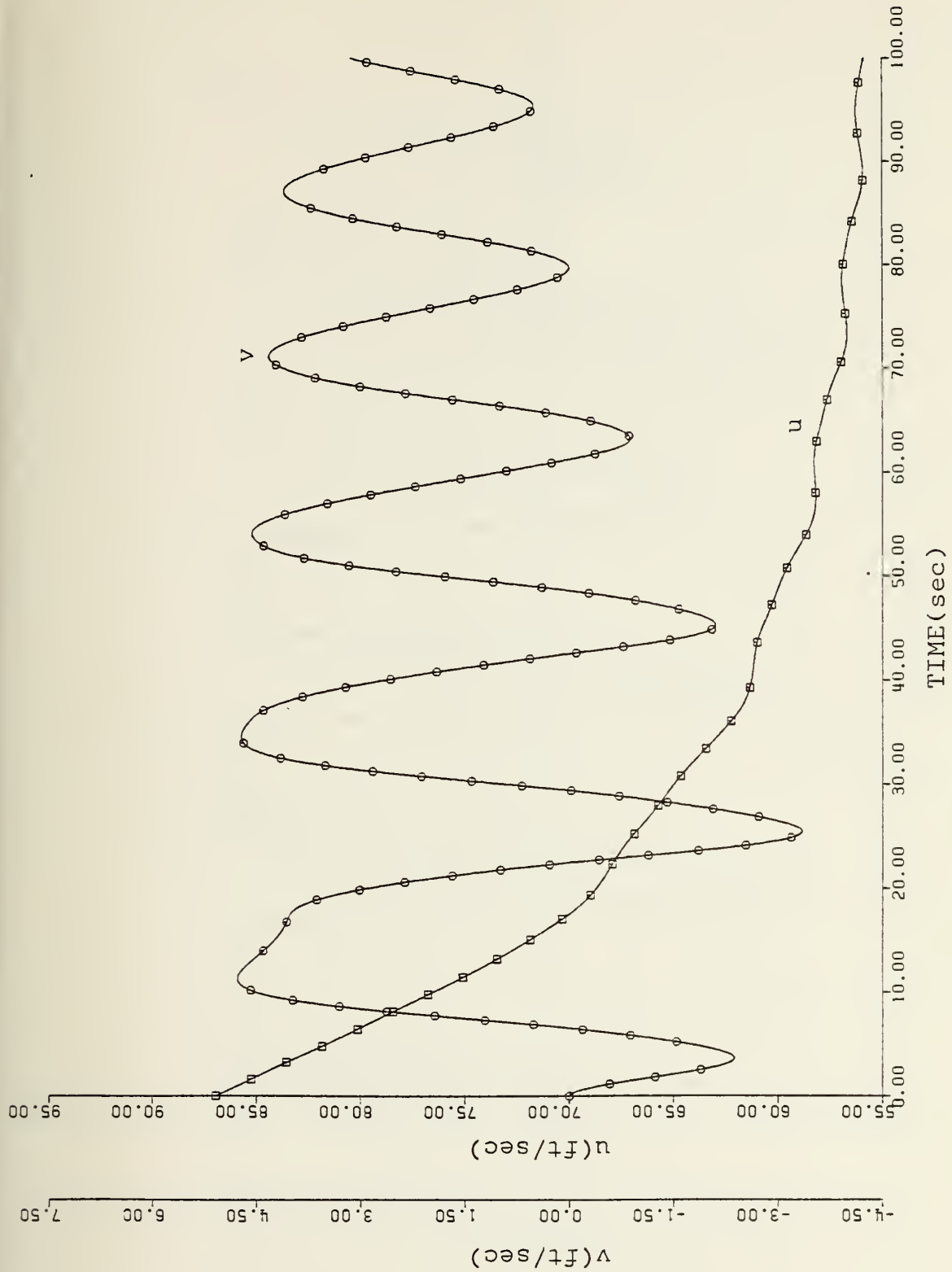


Fig. 22 - Surge and Sway Velocities Vs. Time, Thruster Reversal, Trial and Error Solution

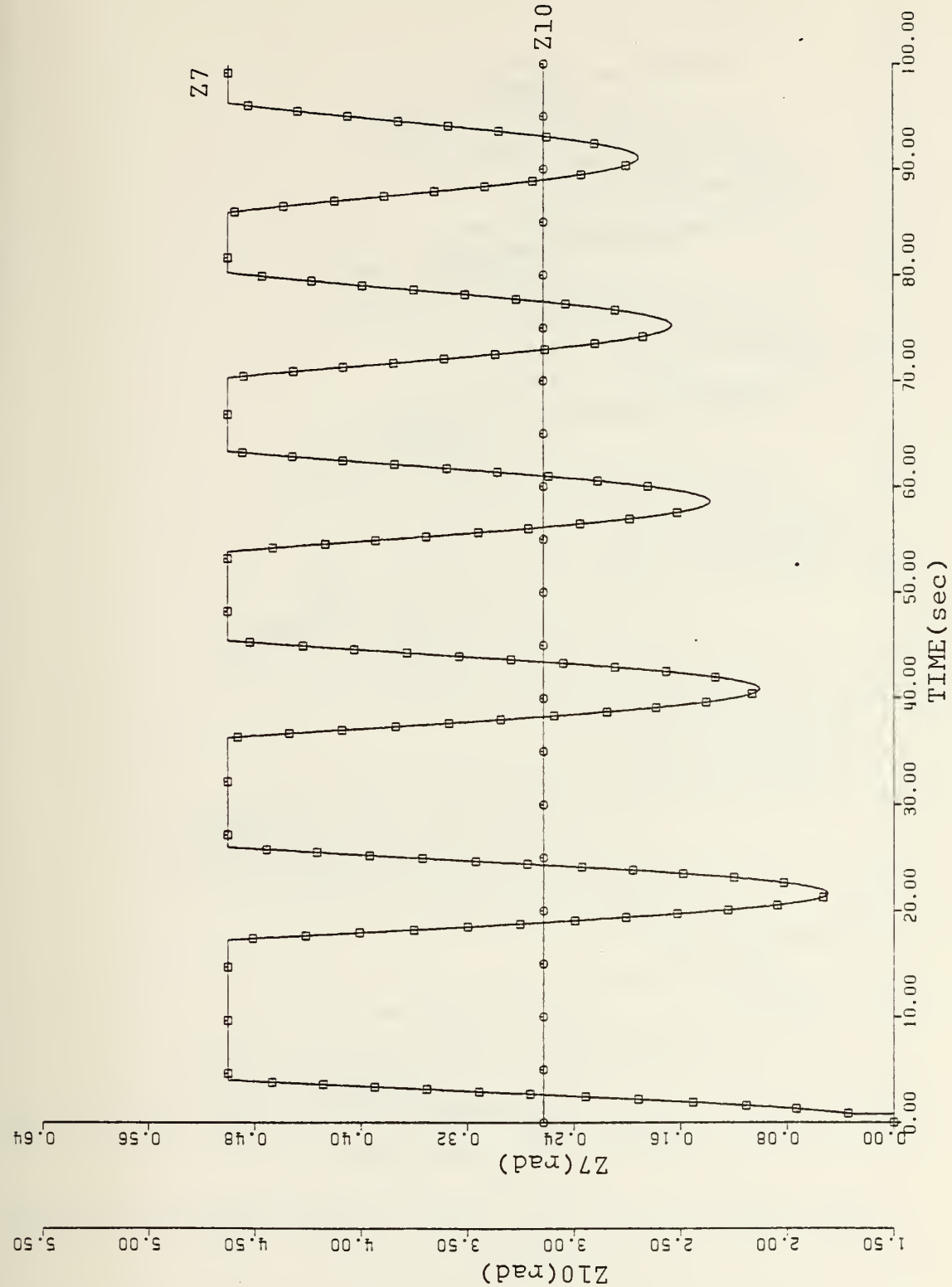


Fig. 23 - Effector Action Vs. Time, Thruster Reversal, Trial and Error Solution

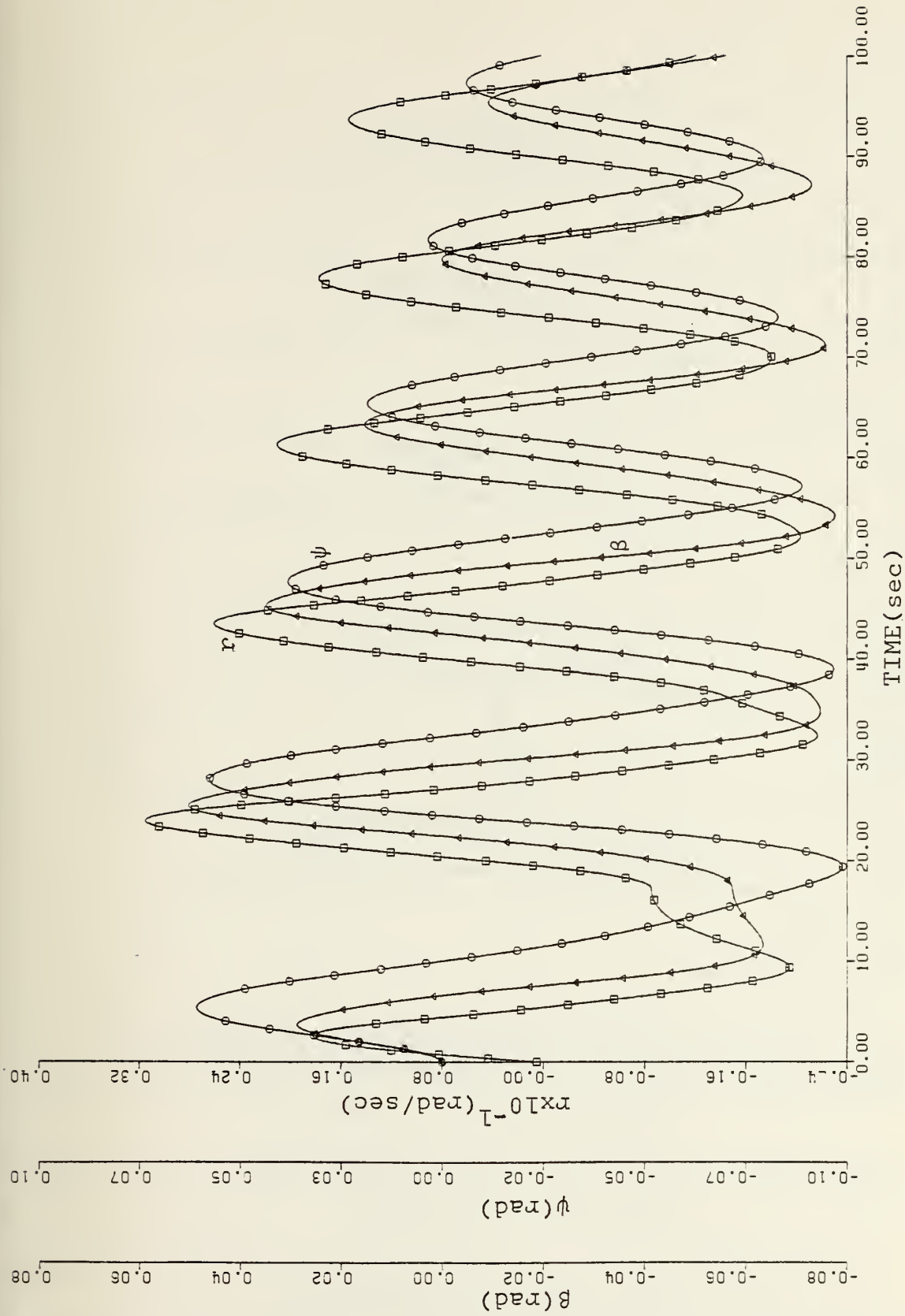


Fig. 24 - Yaw Rate, Heading and Slip Angle Vs. Time, Thruster Reversal, Trial and Error Solution

Fig. 25 - Forward Force, Side Force and Turn Moment Vs. Time, Thruster Reversal, Trial and Error Solution

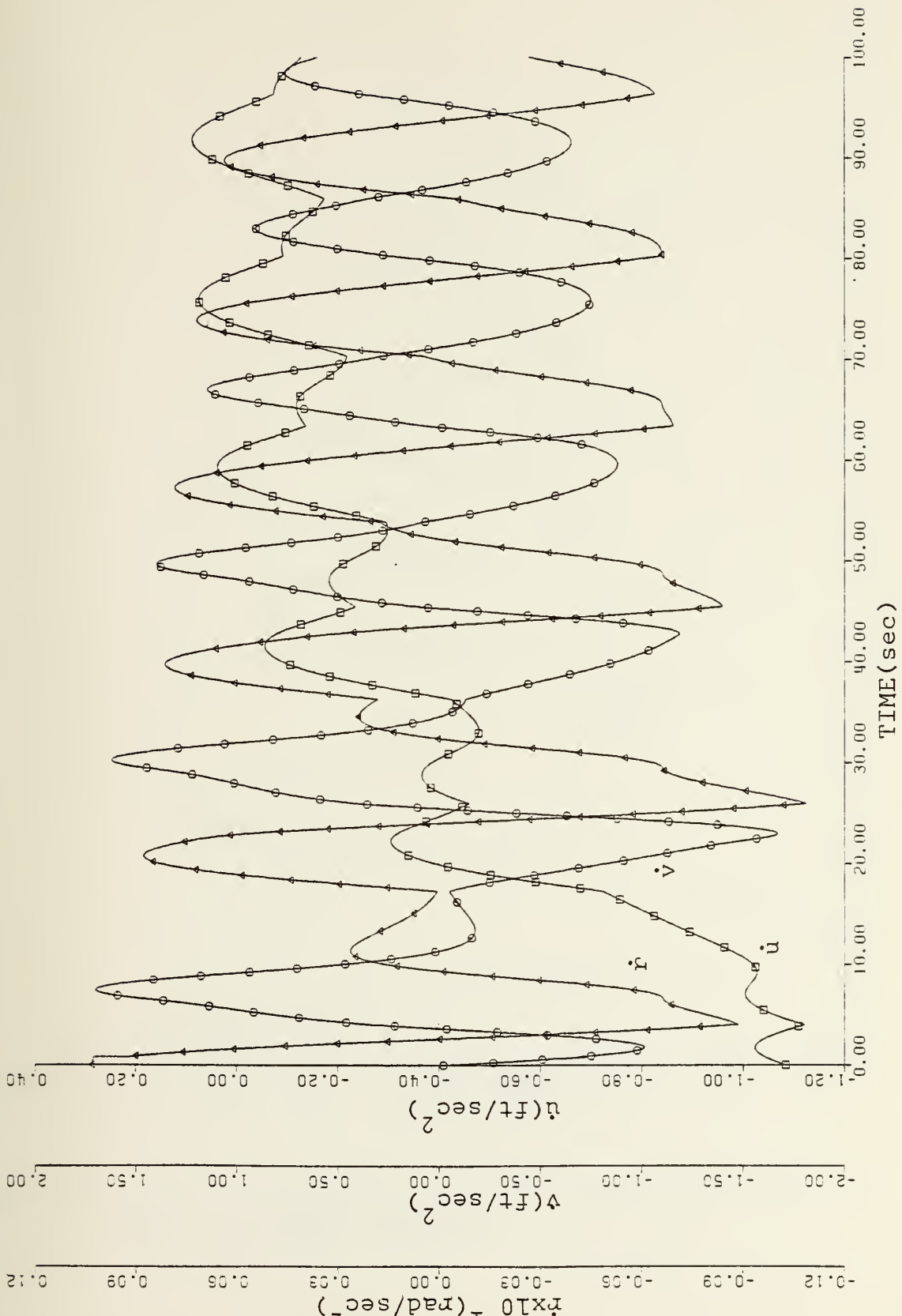


Fig. 26 - Surge, Sway and Yaw Accelerations Vs. Time, Thruster Reversal, Trial and Error Solution

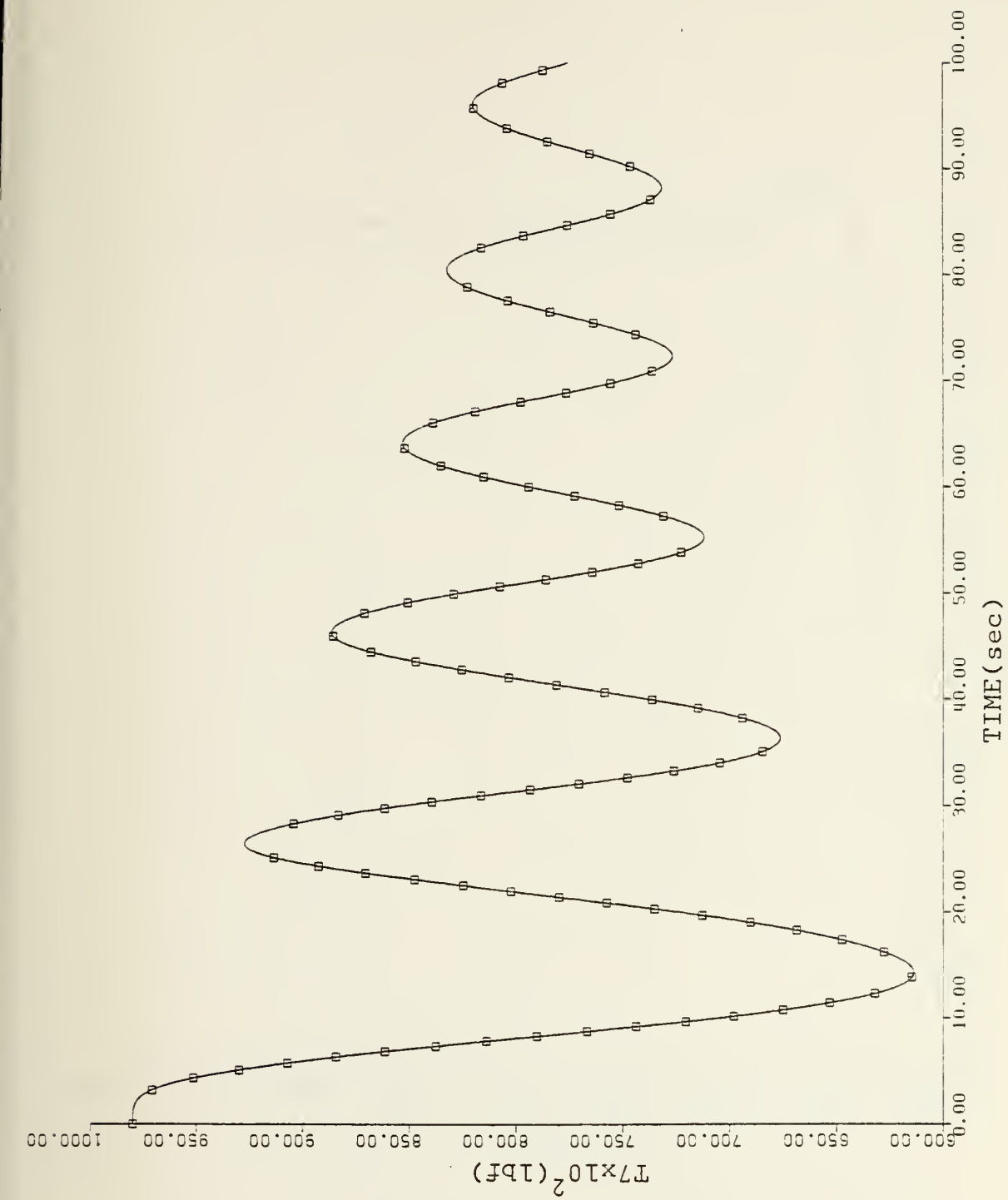


Fig. 27 - Port Thruster Action Vs. Time, Thruster Reversal, Trial and Error Solution

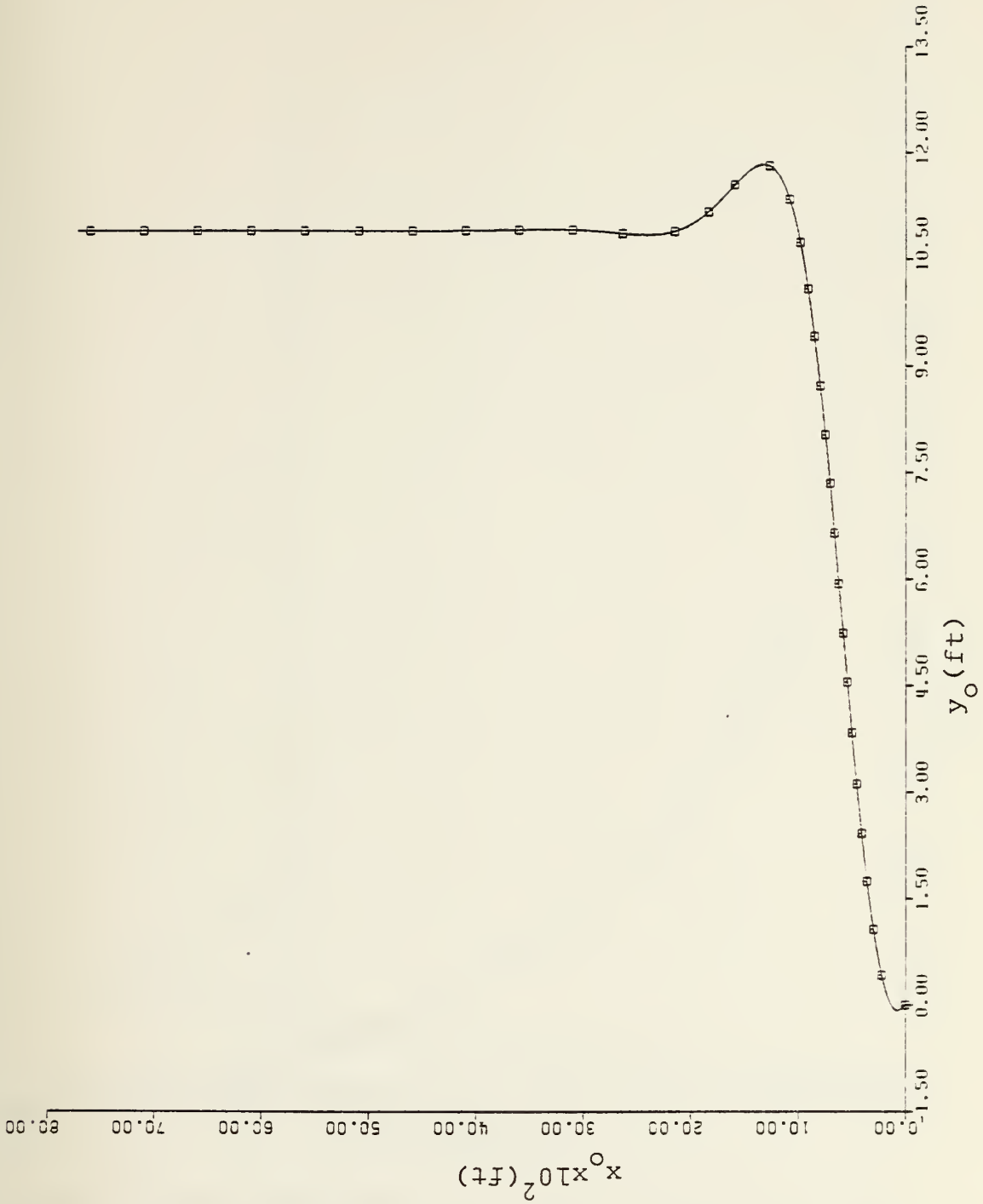


Fig. 28 - Sea Track, Thruster Failure, Optimal Solution

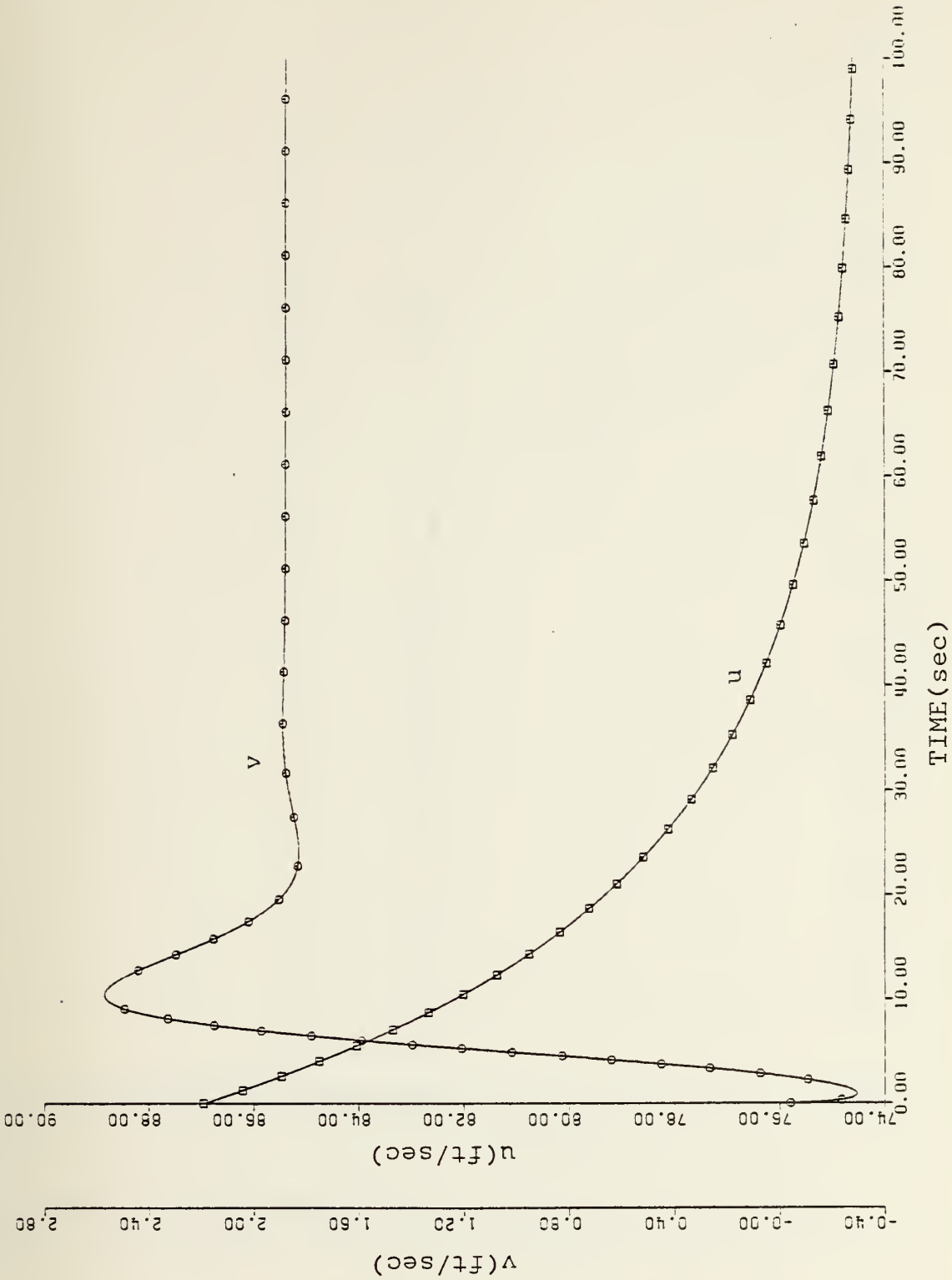


Fig. 29 - Surge and Sway Velocities Vs. Time, Thruster Failure, Optimal Solution

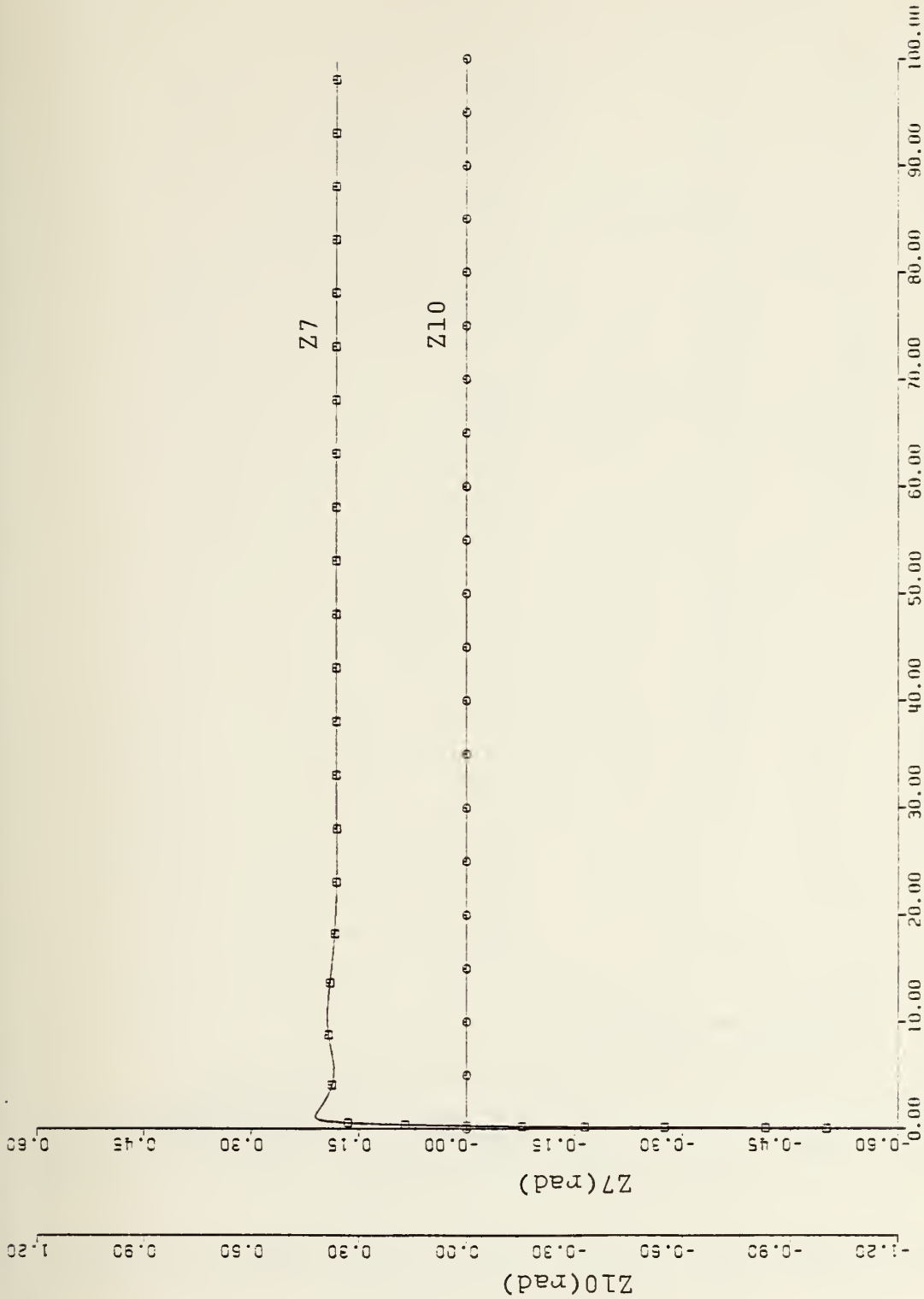


Fig. 30 - Effector Action Vs. Time, Thruster Failure, Optimal Solution

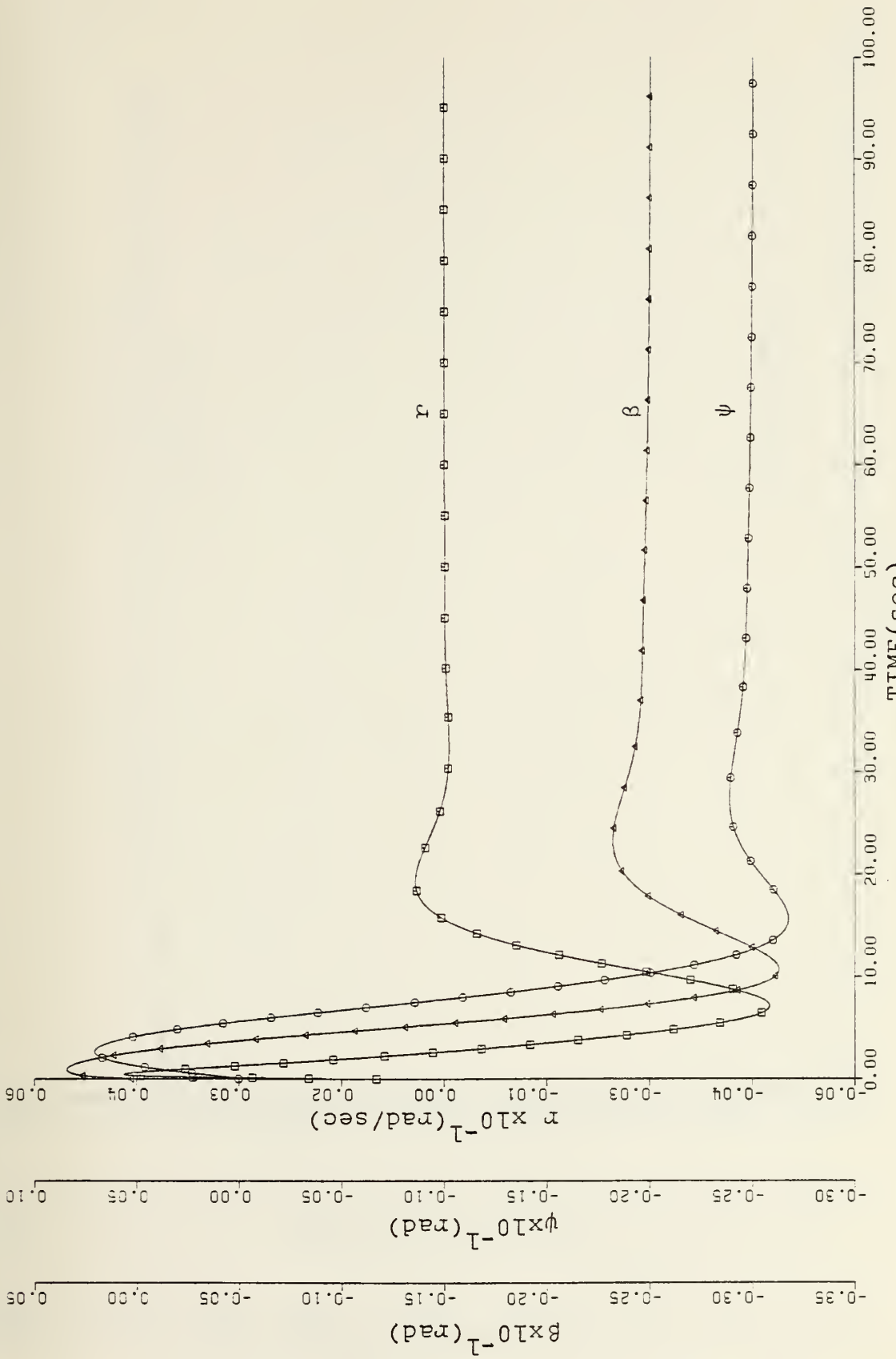


Fig. 31 - Yaw Rate, Heading and Slip Angle Vs. Time, Thruster Failure, Optimal Solution

Fig. 32 - Forward Force, Side Force and Turn Moment Vs. Time, Thruster Failure, Optimal Solution

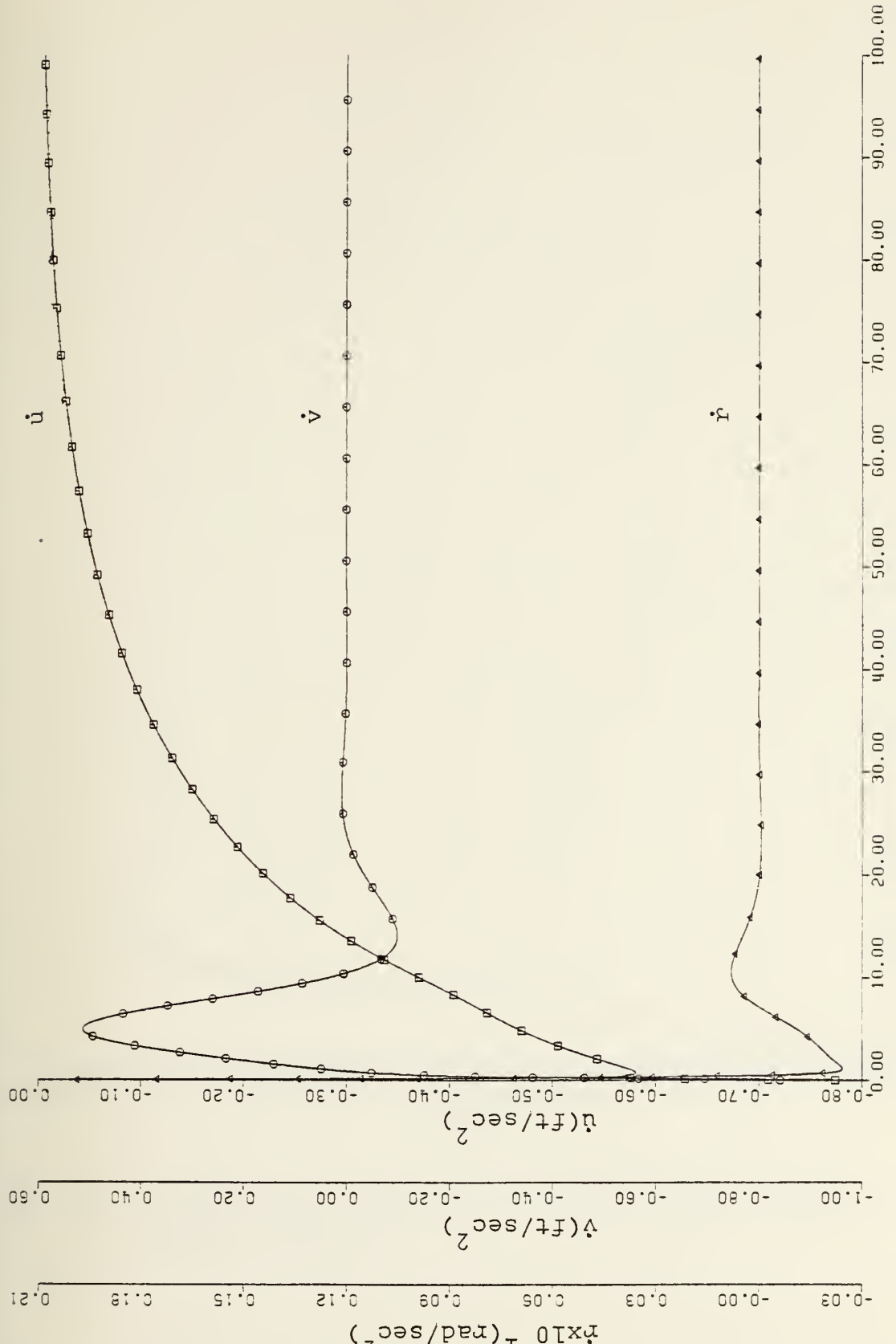


Fig. 33 - Surge, Sway and Yaw Acceleration Vs. Time, Thruster Failure, Optimal Solution


Fig. 34 - Port Thruster Action Vs. Time, Thruster Failure, Optimal Solution

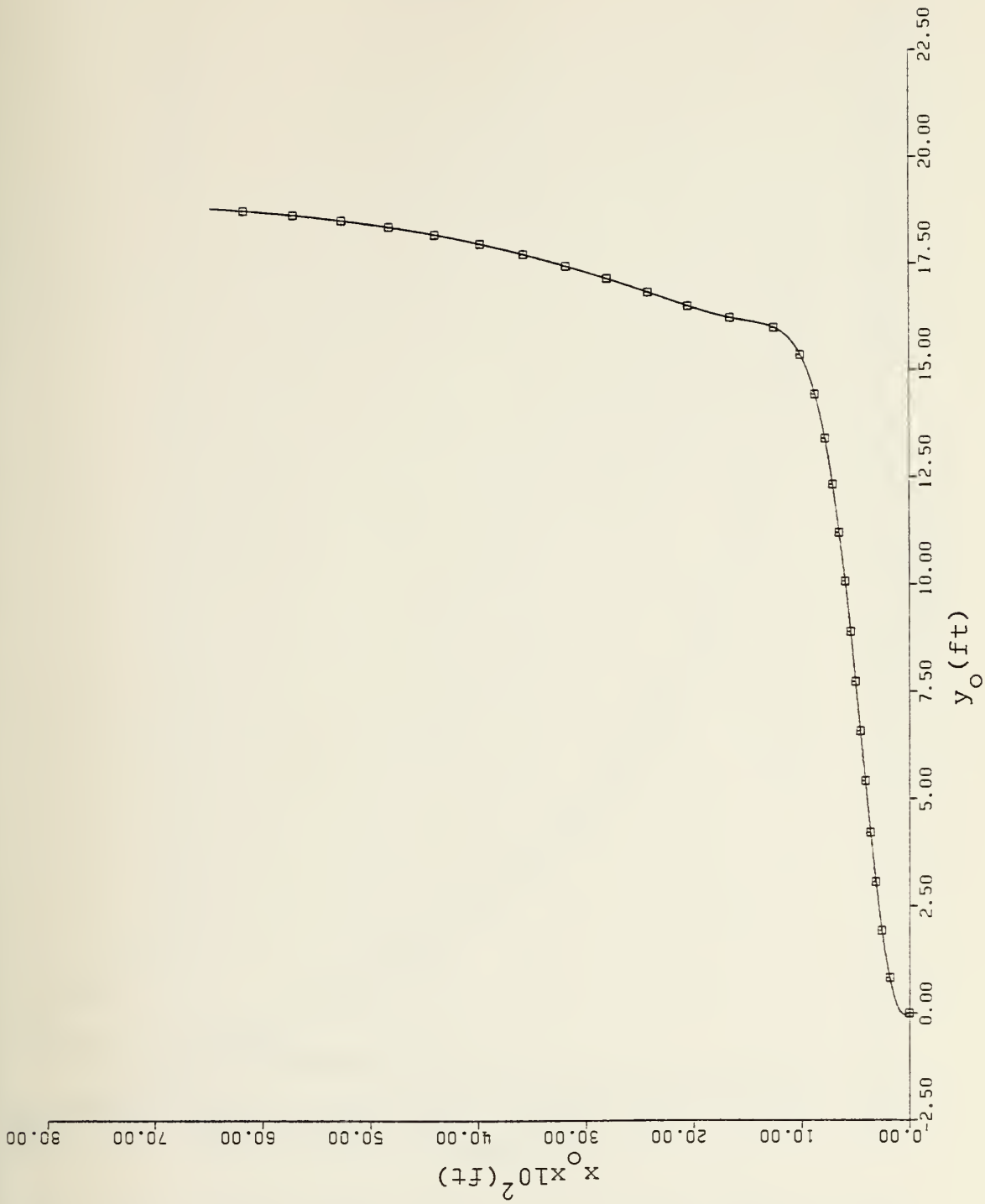


Fig. 35 - Sea Track, Thruster Reversal, Optimal Solution

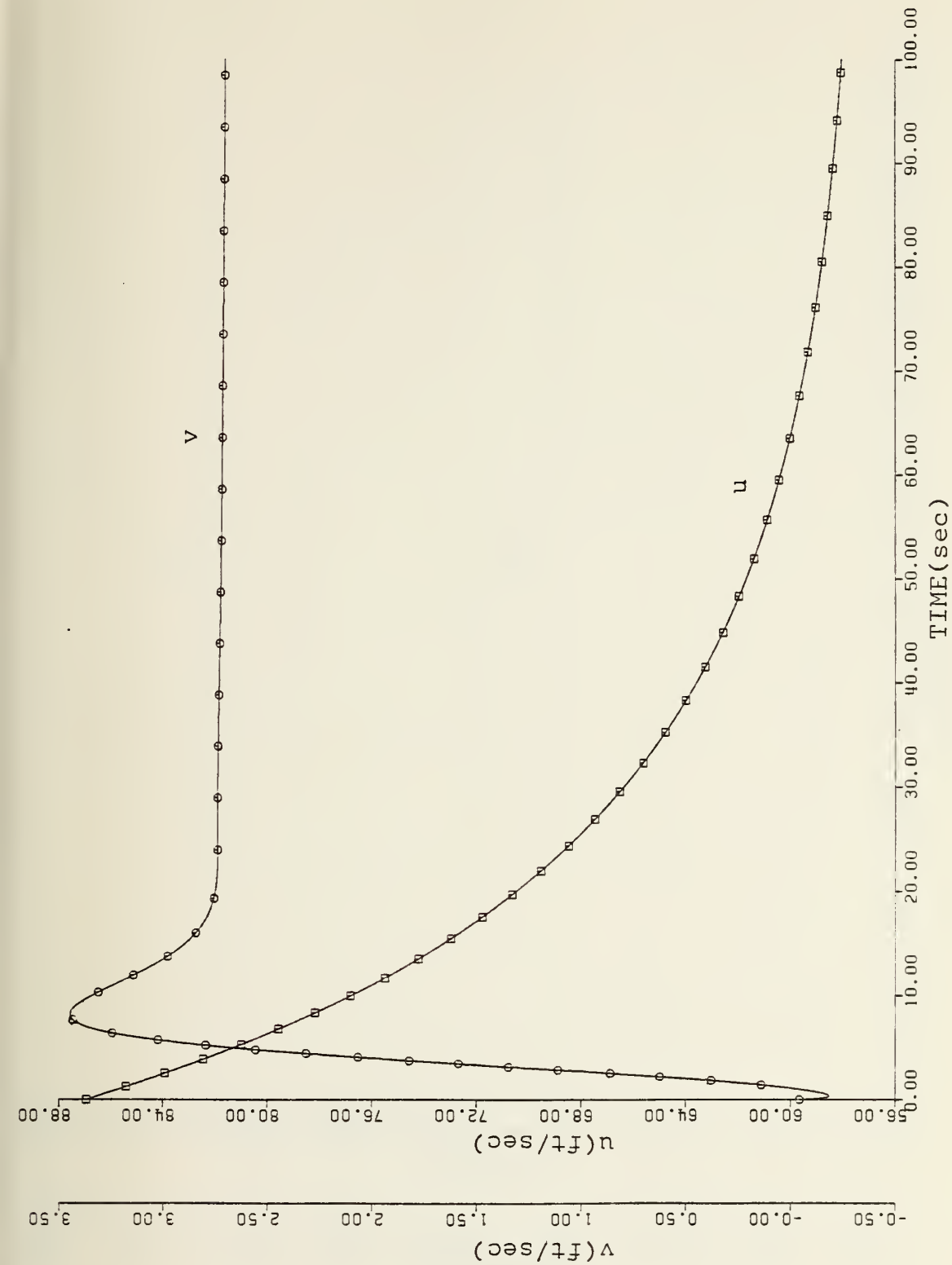


Fig. 36 - Surge and Sway Velocities Vs. Time, Thruster Reversal, Optimal Solution

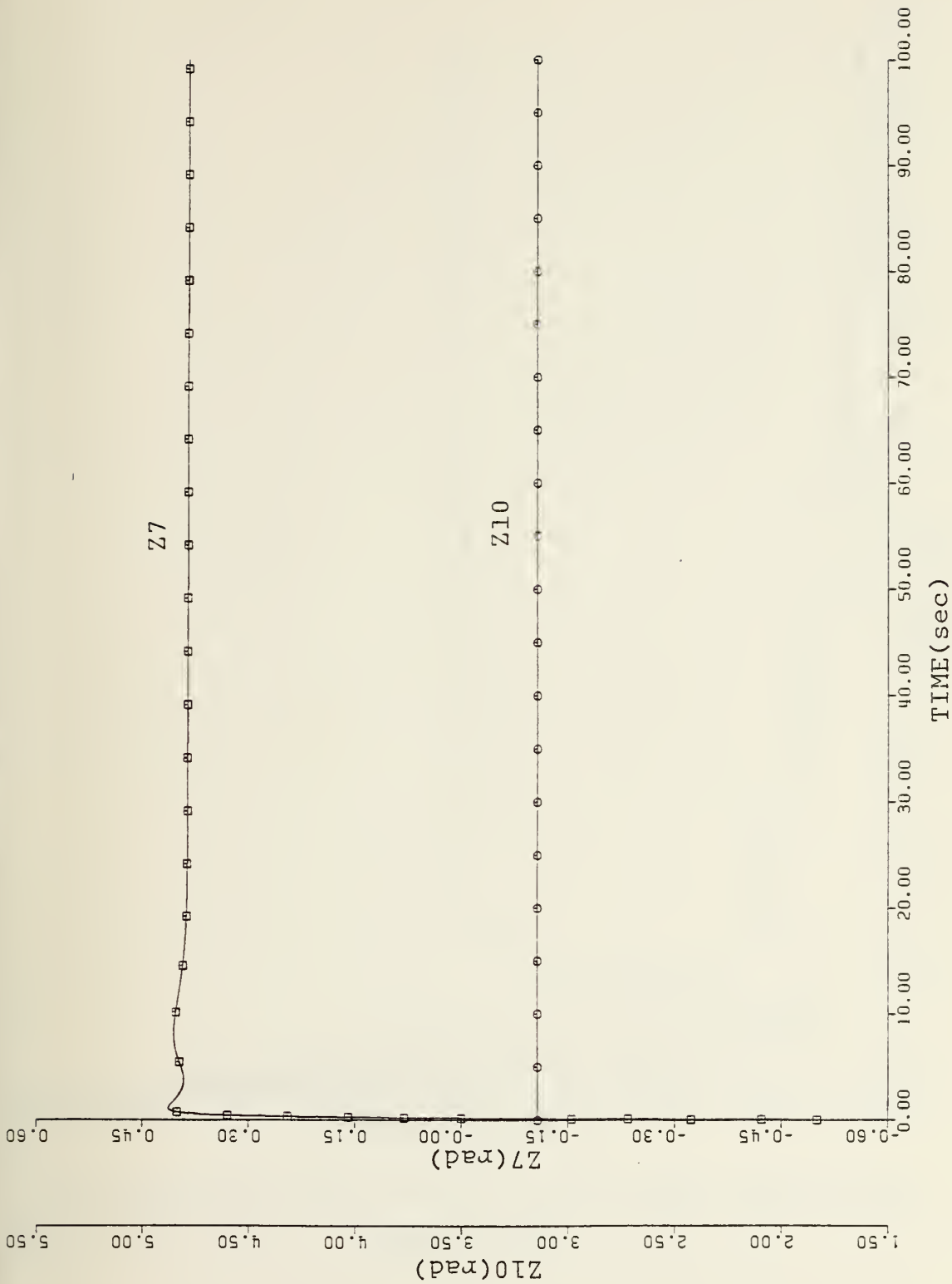


Fig. 37 - Effector Action Vs. Time, Thruster Reversal, Optimal Solution

Fig. 38 - Yaw Rate, Heading and Slip Angle Vs. Time, Thruster Reversal, Optimal Solution

Fig. 39 - Forward Force, Side Force and Turn Moment Vs. Time, Thruster Reversal, Optimal Solution

Fig. 40 - Surge, Sway and Yaw Accelerations Vs. Time, Thruster Reversal, Optimal Solution

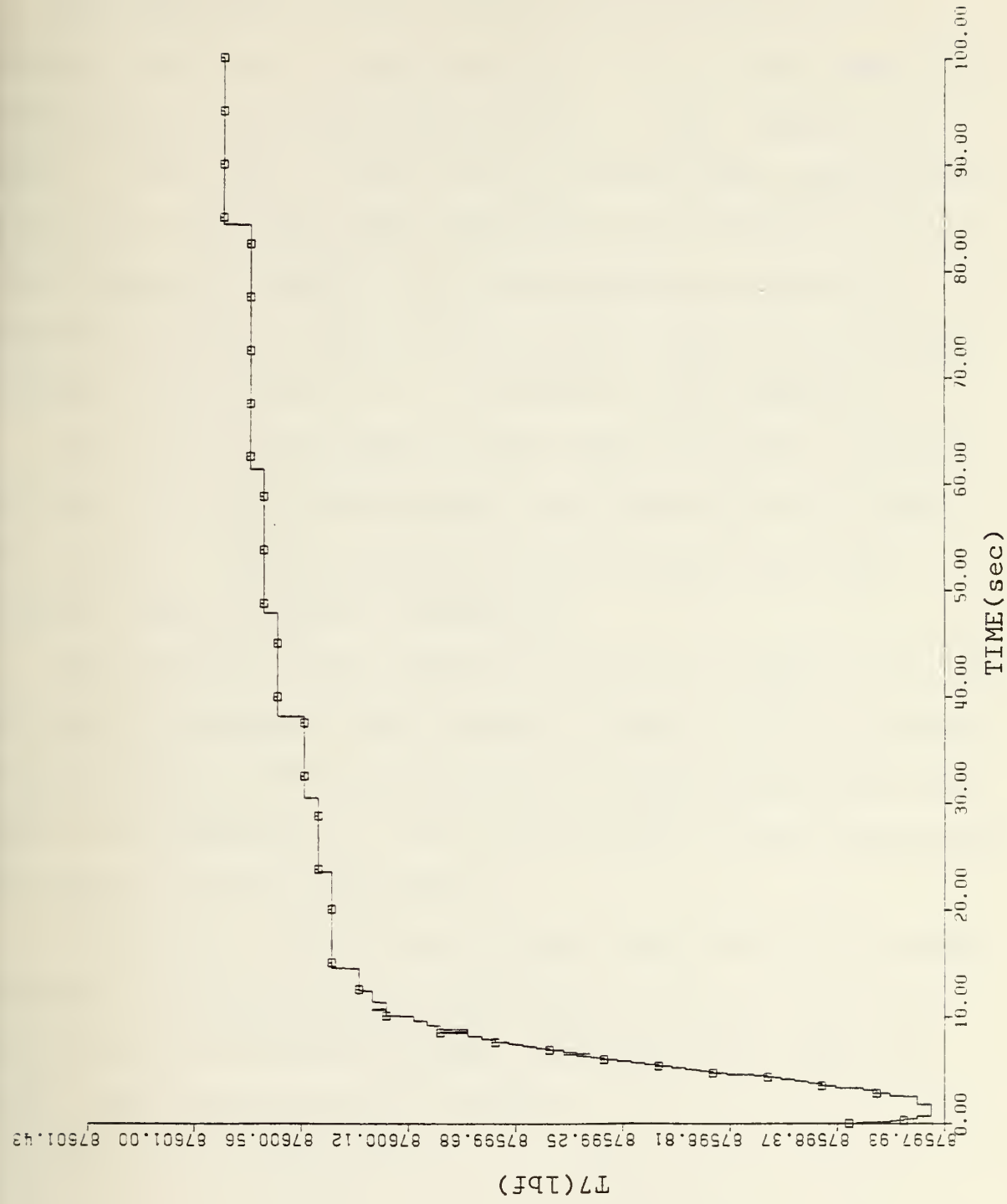


Fig. 41 - Port Thruster Action Vs. Time, Thruster Reversal, Optimal Solution

The sea track (see Fig. 35) of the optimal solution becomes stabilized at approximately 18 feet to the right of the original track (due north), with a slight tendency to drift to the right. This is not of significant consideration due to the relatively small magnitude of drift and the fact that during the conduct of an actual emergency situation proper corrective action would be also taken by the crew of the ship in the first 10 to 15 seconds of the emergency.

It is important to keep in mind that the ship's response for both the trial and error and the optimal solutions was the result of totally automatic operation and any human operator inputs were not considered.

The deviation to the right obtained by the use of the trial and error algorithm at 100 seconds as shown in Fig. 21 has an average value of about 18 feet and is fluctuating around this value by a magnitude of 6 feet which would be more than enough to discrupt normal ship activity.

In addition, the situation is more aggravated when surge, sway and yaw accelerations (see Figs. 26 and 33) are taken into account because even though they are small, they are still significant after 100 seconds.

## C. COMPARISON OF THE OPTIMAL SOLUTION AND THE REAL=TIME HUMAN OPERATOR RESPONSE

As stated in the introduction, a real time simulation of five-degree-of-freedom Surface Effect Ship was available [Ref. 4], utilizing a human operator to input only ganged thruster action, the thrust being constant.

Comparison of the optimal solution and the above mentioned simulation gave the following results during a thrust reversal scenario:

1. Initial recognition of the emergency by the human operator did not occur until approximately three seconds into the emergency, as compared to the optimal solution with an instantaneous recognition of the failure. Consequently, as shown in Table IV, the absolute values of all the outputs reached by a human operator controlled SES are much greater than those observed in the optimal control, given the same initial conditions.

TABLE III

Comparison of Optimal Solution and Human Operator Response

| | HUMAN OPERATOR | OPTIMAL SOLUTION |
|---|---|---|
| Time for first overshoot(sec) | 39 | 22 |
| Deflection from original track (ft) | 100 (worst case) | 18 |
| Time to settle back(sec) | 78 | 35 |
| Final deflection(ft) | 0 | 18 |
| Turn rate(rad/sec) | .007 | .0065 |

Specific examples are as follows:

1. Maximum track deviation obtained by the ship with the optimal control in effect was approximately 18 feet, whereas with the human operator maximum track deviation varied from 35 feet to 100 feet, depending upon operator response and familiarization with the failure as well as the ability of the operator to recognize the onset of an emergency situation through the visual cues provided by the real time simulation.

2. Turn rate was approximately the same, i.e., .007 rads/sec for both situations. However, as might be expected from a human, the turn rate exhibits a much more sinusoidal behavior as compared to the optimal solution which immediately sought and settled down to a steady state value.

3. The state variables under real time simulation showed a more pronounced fluctuation.

4. An advantage of the real time simulation over the optimal solution was that the human operator in all cases, i.e. both thrust failure and thrust reversal, was able to maneuver the ship back to the original track, whereas the optimal solution maneuvered the ship to a parallel track and never returned to the original. This, of course, stems from the method used to find the "steady state" values around which the equations of the system were linearized.

Nevertheless, the difference of 18 feet between the original track and the one that is reached at steady state by the optimal algorithm is not significant compared either to the ship's width (100 feet) or to the tactical considerations of the ship.

D. NONLINEAR VERSUS LINEAR SYSTEM RESULTS

In order to determine how "optimal" the response of the nonlinear system was with the use of the state feedback values obtained from the linear regulator design, a comparison of values of the states and the performance indices were made during a failure.

The results are shown in Table III. As can be easily verified, the differences in steady state values obtained from the linearized system and the nonlinear system are quite small, ranging from .77% to 1.77%, with the exception of the steady state thruster angle (15% difference).

The above results point out that the linear assumptions and approximations used in this study hold quite well over the operating range.

TABLE IV

Comparison of Linear and Nonlinear Models

| | LINEAR | NONLINEAR |
|---|---|---|
| Surge velocity (ft/s) | 75.98 | 74.63 |
| Sway velocity (ft/s) | 1.88 | 1.87 |
| Angular velocity (rad/s) | $.214 \times 10^{-5}$ | $-.211 \times 10^{-5}$ |
| Yaw angle (rad) | -.0248 | -.025 |
| Displacement in x direction (ft) | 7453 | 7342 |
| Displacement in y direction (ft) | 10.762 | 10.88 |
| Steady state thruster angle (rad) | .15256 | .1804 |

# VI. CONCLUSIONS AND RECOMMENDATIONS

## A. CONCLUSIONS

Comparison of the results of all three methods examined leads to the conclusion that the optimal control solution is by far the best one.

Control effort, be it thruster angle or thruster magnitude variation, is less with the optimal control solution. This is of great consideration not only from the aspect of wear and tear of the mechanical parts but also from the point of ship performance as a naval unit, especially since its speed is so far greater than the conventional ships.

Augmentation of human operator control inputs with the optimal solution during failure scenarios presents the best solution in order to maintain positive control of the ship under any operating conditions. This approach would combine the best attributes of the human operator and the optimal control schemes.

## B. RECOMMENDATIONS

Based on the previous analysis, the following could be investigated in the future.

1. A sufficiently complex constrained parameter optimization routine (COPES-CONMIN) can be used to arrive logically at a set of relative system response with respect to physical constraints. This optimization will still be dependent on the performance index selected by the design engineer and his

his ability to calculate explicitly its value for a given dynamic response [Ref. 11].

2. The right-hand side of the equations of motion could be expanded to include more terms to provide an increase in quantitative accuracy of the drag terms such as bubble drag and include also a constant power propulsion plant versus a constant thrust one. This could be done easily since the terms are additive.

3. Development of a computer program to augment the control efforts commanded by a human operator should be investigated, tested and implemented on the RTS5D of Ref. 4.

4. It might prove worthwhile to investigate more closely the trial and error design for improved response characteristics of this method of control.

# APPENDIX A

## LINEAR REGULATOR DESIGN THEORY

Optimal control theory provides a means for utilization of state variable feedback in order to control a system by minimizing a performance index or cost function [Refs. 7 and 8].

Having a linear system defined as $\dot{\underset{\sim}{x}} = \underset{\sim\sim}{A}\underset{\sim}{x} + \underset{\sim\sim}{B}\underset{\sim}{\mu}$ where $\underset{\sim}{\mu}$ is the control input vector, the linear optimal control law is defined as $\underset{\sim}{\mu}_{opt}(t) = -\underset{\sim\sim}{G}\underset{\sim}{x}(t)$.

The assumptions under which this solution is valid are:

1. The control vector is unconstrained.
2. The performance index is defined as

$$J = \int_o^{t_f} \{\underset{\sim}{x}^T \underset{\sim\sim}{Q}\underset{\sim}{x} + \underset{\sim}{\mu}^T \underset{\sim\sim}{R}\underset{\sim}{\mu}\}\, dt$$

where $\underset{\sim}{Q}$ is a positive semidefinite or positive definite real symmetric matrix and $\underset{\sim}{R}$ is a positive definite real symmetric matrix. The matrices $\underset{\sim}{Q}$ and $\underset{\sim}{R}$ determine the relative importance of the square of the error and energy expenditure during the transient period.

3. The system is controllable and state observable.

With these assumptions, substitution for $\underset{\sim}{\mu}$ leads to

$$J = \int_o^{t_f} (\underset{\sim}{x}^T \underset{\sim\sim}{Q}\underset{\sim}{x} + \underset{\sim}{G}(t)^T \underset{\sim}{x}^T \underset{\sim}{R}\, \underset{\sim}{G}(t)\underset{\sim}{x})\, dt$$

$$J = \int_o^{t_f} \{\underset{\sim}{x}^T (\underset{\sim}{Q} + \underset{\sim}{G}(t)^T \underset{\sim}{R}\, \underset{\sim}{G}(t))\underset{\sim}{x}\}\, dt$$

The matrix $\underset{\sim}{G}(t)$ is found to be

$$\underset{\sim}{G}(t) = \underset{\sim}{R}^{-1}\underset{\sim}{B}^{T}\underset{\sim}{P}(t)$$

Here $\underset{\sim}{P}(t)$ satisfies the matrix Riccati equation

$$\dot{\underset{\sim}{P}}(t) + \underset{\sim}{Q} - \underset{\sim}{P}(t)\ \underset{\sim\sim}{B}\underset{\sim}{R}^{-1}\underset{\sim}{B}^{T}\underset{\sim}{P}(t) + \underset{\sim}{P}(t)\underset{\sim}{A} + \underset{\sim}{A}^{T}\underset{\sim}{P}(t) = 0$$

subject to the boundary condition $\underset{\sim}{P}(tf) = 0$.

The elements of the matrix $\underset{\sim}{G}(t)$ are referred to as the feedback coefficients, since the optimal control consists of a time-weighted linear combination of the state variables.

This result is important since it indicates that in an optimal system all the state variables are to be fed back, not only the output, as it is customary in classical control theory. A graphical representation of this optimal system is presented in Fig. 42.

The Riccati equation is integrated backwards in time from the known terminal condition $P(\infty) = 0$ until the desired degree of accuracy is reached. When the final time approaches infinity, the $\underset{\sim}{P}$ matrix becomes constant, thereby simplifying its determination.

As can be seen for the previous presentation, a different linear optimal control is generated for every relative set of weighting matrices, $\underset{\sim}{Q}$ and $\underset{\sim}{R}$, provided. Additionally, the system response is optimal in a mathematical sense only, since no assurance on acceptable system overshoots and input peak values can be guaranteed.

A minimum area could have an excessive peak which would

provide a physically unrealizable control scheme. The design synthesis thus requires an initial guess at the relative importance multipliers, followed by subsequent adjustments based on time simulation of the controlled system dynamics .

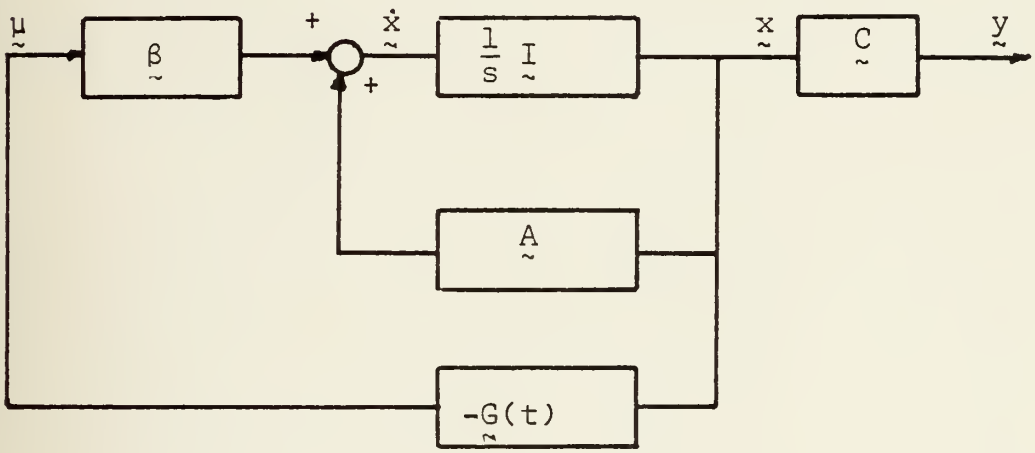


Fig. 42

```
// EXEC CSMPXV
//X.SYSIN DD *
PARAMETER XXXX=1.
INITIAL
       IA=0.
       L=87.
       V=0.
       R=C.
       XC=C.
       YO=0.
       Z=C.
DYNAMIC
NOSORT
       T=392CCC.
       TMAX=392CCC.
       T7MAX=98CCC.
       T8MAX=98CCC.
       T9MAX=98CCC.
       T10MAX=98CCC.
       AM=17C364.
       CDX=50.33
       CDY=14544.
       RZ=9527CCCCC.
       CO=110.8
       WW=26.C38
       A22=1.
       CDZP=13336.698
       A33=294118.
       CDP=9.174
       FB=240.
       WB=1CC.
       LD=3.
       L3=100.
       LP=5.
       LZ=30.
       A34=588236.
       RY=815899CC.
       RX=1822CCCCC.
       S1=50.
       S2=5C.
       S3=50.
       S4=5C.
       Z1=2.
       Z2=0.5
       Z3=-C.5
       Z4=0.03
       Z5=-0.C3
       Z6=-.C5
```

```
      Z11=3.1416
      Z12=C.2
      RHC=2.0
      G=32.2
      ZAB=3.1416
      PCTK1=1.
      PCTK3=1.
      PCTK4=1.
      PCTK6=1.
      PCTK5=1.
      AAPCT=ABS(PCTK5)
      IF(AAPCT.GT..1)GO TO 207C
      Z=C.
      Z7=Z
      Z8=Z
      Z9=Z
      Z1C=Z
      GO TO 744
  744 CONTINUE
      IF(Z.GT.Z2)GO TO 79C
      IF(Z.LT.Z3)GO TO 791
      IF(Z.GT.Z4)GO TO 792
      IF(Z.LT.Z5)GO TO 792
      Z=C.C
      Z7=C.
      Z8=0.
      Z9=0.
      Z1C=C.
      GO TO 792
  79C Z=Z2
      Z7=Z2
      Z8=Z2
      Z9=Z2
      Z10=Z2
      GO TO 792
  791 Z=Z3
      Z7=Z3
      Z8=Z3
      Z9=Z3
      Z10=Z3
      GO TO 792
2C7C CONTINUE
      Z=.14-.C316*(U-74.422)+.684*(V-1.86)+185.7*(R+.000008)...
      +110.7*(PSI+.0254)+.186*(YO-10.88)
2CC CONTINUE
  501 CONTINUE
      Z7=Z
      Z8=Z
```

```
      Z9=Z
      Z1C=ZAE*PCTK5
      IF(Z.GT.Z2)GC TO 2075
      IF(Z.LT.Z3)GC TO 2076
      IF(Z.GT.Z4)GO TO 792
      IF(Z.LT.Z5)GC TO 792
      Z=C.
      Z7=0.
      Z8=C.
      Z9=C.
      Z1O=ZAE*PCTK5
      GO TC 792
2075  Z=Z2
      Z7=Z2
      Z8=Z2
      Z9=Z2
      Z1O=ZAE*PCTK5
      GO TC 792
2076  Z=Z3
      Z7=Z3
      Z8=Z3
      Z9=Z3
      Z1O=ZAE*PCTK5
      GO TC 792
 792  CONTINUE
 622  CONTINUE
      IF(IA.LT..5) GO TO 33C
      FAIL=0.C
 33C  CONTINUE
      T7=87600.*(1.-.00046*(R+.000008)-.0007*(PSI+.0254))
      T8=T8MAX*(1.+POTK3)/2.
      T9=T9MAX*(1.+POTK4)/2.
      T10=T10MAX*(1.+POTK6)/2.
      T7C=T7*CCS(Z7)
      T8C=T8*CCS(Z8)
      T9C=T9*CCS(Z9)
      T1CC=T1C*CCS(Z10)
      T7S=T7*SIN(Z7)
      T8S=T8*SIN(Z8)
      T9S=T9*SIN(Z9)
      T10S=T10*SIN(Z10)
      TFCRW=T7C+T8C+T9C+T10C
      TSIDE=T7S+T8S+T9S+T1CS
      TYAW=(T7C*S4)+(T8C*S3)-(T9C*S1)-(T10C*S2)-(T7S*CO)-(T8S*CO)...
      -(T9S*CC)-(T10S*CC)
      T=T7+T8+T9+T1C
      C=(-1.)*YC
      IF(T.GT.TMAX)GO TC 793
```

```
      IF(T.LT.0.0)GO TO 794
      GO TO 795
  793 T=TMAX
      GO TO 795
  794 T=0.0
      GO TO 795
  795 CONTINUE
      UDOT=(((-1.0)*CDX/AM)*U*L)+(TFORW/AM)+V*R
      VDOT=(TSIDE/AM)-(((CDY/AM)*V*ABS(V))-U*R
      RDOT=(((CDY/RZ)*WW*V*ABS(V))+(TYAW/RZ)+(A22*U*V*(WW/RZ))
      BETA=ATAN(-V/L)
      VS=(((U*L)+(V*V))**.5
      XODOT=L*COS(PSI)-V*SIN(PSI)
      YODOT=L*SIN(PSI)+V*COS(PSI)
      L=L+.025*UDOT
      V=V+.025*VDOT
      R=R+.025*RDOT
      PSI=PSI+.025*R
      XO=XO+.025*XODOT
      YO=YO+.025*YODOT
TIMER FINTIM=100.,DELT=.025,PRDEL=.025,OUTDEL=.025
OUTPUT YO,XO
   LABEL SEA TRACK(STBD THRUSTER REVERSAL)
OUTPUT TIME,Z7,Z10
   LABEL EFFECTOR ACTION(STBD THRUSTER REVERSAL)
OUTPUT TIME,TFORW,TSIDE,TYAW
   LABEL FWD FORCE/SIDE FORCE/TURN MOMENT(STBD THRUSTER FAILURE)
OUTPUT TIME,T7
   LABEL PORT THRUSTER ACTION(STBD THRUSTER FAILURE)
OUTPUT TIME,UDOT,VDOT,RDOT
   LABEL SURGE/SWAY/YAW ACCELERATION(STBD THRUSTER FAILURE)
OUTPUT TIME,R,PSI,BETA
   LABEL YAW RATE/HEADING/SLIP ANGLE(STBD THRUSTER FAILURE)
OUTPUT TIME,U,V
   LABEL SURGE/SWAY VELOCITY(STBD THRUSTER FAILURE)
         PAGE XYPLOT
END
STOP
```

```
// EXEC CSMFXV
//X.SYSIN DD *
PARAMETER XXXX=1.
INITIAL
       X1=12.578
       X2=0.
       X3=0.
       PSI=0.
       XO=0.
       YO=0.
DYNAMIC
NOSORT
       LSS=74.422
       VSS=1.86
       RSS=-.000018
       Z7SS=.14
       T7SS=87600.
       CDX=50.33
       CDY=14944.
       M=170364.
       A22=1.
       IZ=9927000000.
       CO=110.8
       WW=26.038
       T8SS=98000.
       T9SS=98000.
       T10SS=0.
       S4=50.
       L=X1+LSS
       V=X2+VSS
       R=X3+RSS
       A=-2.*CDX*LSS/M
       B=-2.*CDY*VSS/M
       C=A22*VSS*WW/IZ
       C1=1044.
       ALG=-.14
       C2=ALG
       D=(2.*CDY*VSS+A22*USS)*WW/IZ
       T=TIME
       E=(S4-Z7SS*CO)/IZ
       F=CO*(T7SS+T8SS+T9SS+T10SS)/IZ
       T7=98000.-C1
       X1DOT=A*X1+RSS*X2+VSS*X3+C1/M
       X2DOT=-RSS*X1+B*X2-LSS*X3+Z7SS*C1/M
       X3DOT=C*X1+D*X2+E*C1-F*C2
       PSIDOT=R
       XODOT=L*COS(PSI)-V*SIN(PSI)
       YODOT=L*SIN(PSI)+V*COS(PSI)
```

```
        X1=X1+.C25*X1DOT
        X2=X2+.C25*X2DOT
        X3=X3+.C25*X3DOT
        PSI=PSI+.C25*PSIDOT
        XO=XO+.C25*XODOT
        YO=YC+.C25*YCDOT
        BETA=ATAN(((-1.)*V)/L)
TIMER  FINTIM=10C.,DELT=.025,PRDEL=.025,OUTDEL=.025
OUTPUT T,YC,L,V,R,PSI,XO
END
STOP
```

# LIST OF REFERENCES


1. Oceanics Incorporated Report No. 71-84B, A Study of Surface Effect Ship (SES) Craft Loads and Motions, Part II-Habitability and Maneuverability of SES Craft, by P. Kaplan, J. Bentson and T.P. Sargent, August 1971.

2. Rohr Marine Incorporated Report No. E05P, 3KSES Ship Control System Design Information Report, Vol. I, by A. Greensite, L. Pascoe and M. Wiemer, 24 July 1978.

3. Rohr Marine Incorporated Report No. E03L, Stability and Maneuverability Report, by E. E. Price, E. C. Stoner and N. L. Wener, 30 August 1978.

4. Nelson, T. S., Real Time Simulation of the 5 Degree-of-Freedom 3000 Ton Surface Effect Ship, M. S. Thesis, Naval Postgraduate School, Monterey, 1979.

5. Naval Postgraduate School Report No. NPS62-79-008, Development of a Real-Time Hybrid Computer Simulation for the 3K-SES, 5 DOF, Data-Based Program, Part I-Familiarization and Planning, by A. Gerba, Jr. and G. J. Thaler, June 1979.

6. Manoussos, S., M-D, Added Mass Effect on the Turning Characteristics of the XR-3 SES, paper presented as term project for EE4418 to Professor G. J. Thaler, Naval Postgraduate School, Monterey, California, June 1979.

7. Kirk, D. E., Optimal Control Theory-An Introduction, Prentice-Hall Inc., 1970.

8. Desjardins, B., A User's Manual for Linear Control Programs on IBM/360, M.S. Thesis, Naval Postgraduate School, Monterey, California., 1979.

9. Melsa, J. L. and Jones, S. K., Computer Programs for Computational Assistance in the Study of Linear Control Theory, 2d ed., McGraw-Hill, 1973.

10. Schultz, D. G. and Melsa, J. L., State Functions and Linear Control Systems, McGraw-Hill, 1967.

11. Dundics, M. J., CONSYN-An Optimal Integral Controller Design and Analysis Program, M. S. Thesis, Naval Postgraduate School, Monterey, California, 1977.

INITIAL DISTRIBUTION LIST

| | | No. Copies |
|---|---|---|
| 1. | Defense Technical Information Center<br>Cameron Station<br>Alexandria, Virginia 22314 | 2 |
| 2. | Library, Code 0142<br>Naval Postgraduate School<br>Monterey, California 93940 | 2 |
| 3. | Department Chairman, Code 62<br>Department of Electrical Engineering<br>Naval Postgraduate School<br>Monterey, California 93940 | 1 |
| 4. | Professor A. Gerba, Jr., Code 62Gz<br>Department of Electrical Engineering<br>Naval Postgraduate School<br>Monterey, California 93940 | 5 |
| 5. | Professor G. J. Thaler, Code 62Tr<br>Department of Electrical Engineering<br>Naval Postgraduate School<br>Monterey, California 93940 | 3 |
| 6. | Hellenic Navy Command<br>Holargos<br>Athens, Greece | 4 |
| 7. | Lieutenant Spyridon M-D Manoussos, H.N.<br>1, Iofontos Str.<br>Athens, Greece | 1 |